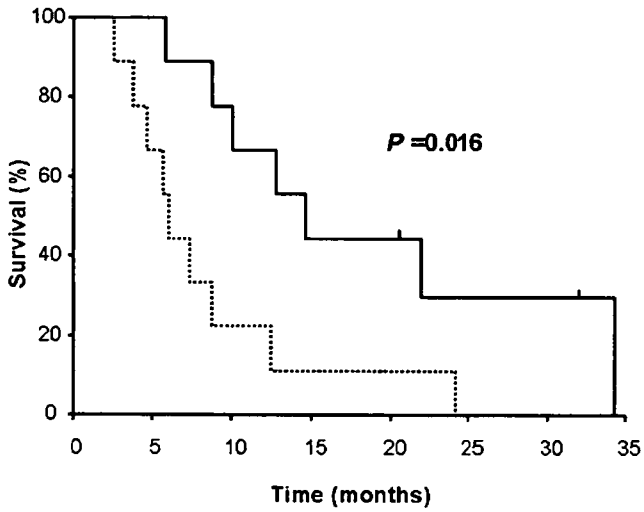

FIGURE 8 – Overall survival after gemcitabine treatment of 18 recurrent pancreatic cancer patients for RRM1 mRNA expression levels. Solid line: low RRM1 expression group (n = 9). Dotted line: high RRM1 expression group (n = 9). Log-rank test = 5.78, p =0.016.

has suggested that *in vivo* induction of resistance to gemcitabine should result in increased expression of RRM1.[13] These data are consistent with the present findings, although they only suggested an association of gemcitabine resistance with higher RRM1 expression. More important was the clear demonstration in the present study of the direct association of RRM1 with gemcitabine resistance through RRM1-specific RNAi treatment. However, the precise mechanisms how the increased expression of RRM1 acts in gemcitabine resistance still remain obscure. In the *in vitro* study with acquired gemcitabine resistant MiaPaCa2-RG and PSN1-RG cells, increase expression of RRM1 was not likely correlated with the increase of cellular resistance to gemcitabine. Although gemcitabine-resistance of PSN1-RG cells was almost equal to that of MiaPaCa2-RG cells, RRM1 expression level was much higher in MiaPaCa2-RG than in PSN1-RG cells. Other molecules involving gemcitabine or 5-FU metabolism or molecules such as p8[38] may be participated in gemcitabine resistance. Further studies are needed to clarify these points.

Although association of the increased expression of RRM1 gene with gemcitabine resistance has been reported based on *in vitro* and *in vivo* acquired gemcitabine resistant tumor cells[12,13] as in the present study, the mechanisms under RRM1 upregulation of resistant cells have not been fully elucidated. Polymorphisms[39] and amplified gene copy number[40] in the RRM1 gene are supposed to be related to the gemcitabine chemoresistance of tumor cells. Gene mutation or epigenetic mechanism such as methylation may influence the expression of RRM1 in resistant cells. Our preliminary experiments, however, did not show any mutational or polymorphic changes in the RRM1 gene between parental and gemcitabine resistant selected cells. Demethylation agents such as 5-aza-2′-deoxycytidine did not change RRM1expression in gemcitabine resistant cells. Future studies for the regulation of RRM1expression could therefore be helpful to obtain modulation of gemcitabine sensitivity in pancreatic cancer cells.

Because the present findings on RRM1 as a factor in gemcitabine resistance are based on an *in vitro* acquired gemcitabine resistant model as shown in the previous studies,[12] it is still unclear whether or not RRM1 should be one of the key molecules involved in the intrinsic resistance to gemcitabine. However, in *in vitro* analysis with human pancreatic cancer cell lines, RRM1 mRNA expression levels are significantly associated with gemcitabine sensitivity in 5 pancreatic cancer cell lines, while increased expression of RRM1 was not likely correlated with the increase of cellular resistance to gemcitabine between acquired gemcitabine resistant MiaPaCa2-RG cells and PSN1-RG cells. Furthermore, clinical data from patients treated with gemcitabine may indicate that RRM1 should play an important role in the intrinsic resistance to gemcitabine. Gemcitabine was more effective to recurrent tumors in those patients with low RRM1 mRNA expression in the tumor obtained at surgery, although expression levels of recurrent tumors were supposed to reflect those of primary tumors. Therefore, patients with low RRM1 mRNA expression might have a significantly longer survival than those with a high expression as previously reported in lung cancer patients[41,42] even though the survival of recurrent pancreatic cancer patients is generally poor. Although our data do not rule out that other molecules of gemcitabine resistance determine intrinsic or acquired sensitivity to gemcitabine *in vivo* as reported in the recent study, the clinical results should be the most feasible for further investigations.

In conclusion, we have demonstrated in the present study that RRM1 should be a key molecule in gemcitabine resistance in pancreatic cancer through both *in vitro* and clinical models. In the continuous struggle to overcome the chemoresistance of pancreatic cancer, RRM1 may have the potential to play the role of a predictor of gemcitabine resistance and modulator of gemcitabine treatment.

References

1. Li D, Xie K, Wolff R, Abbruzzese JL. Pancreatic cancer. Lancet 2004;363:1049–57.
2. Burris HA, III, Moore MJ, Andersen J, Green MR, Rothenberg ML, Modiano MR, Cripps MC, Portenoy RK, Storniolo AM, Tarassoff P, Nelson R, Dorr FA, et al. Improvements in survival and clinical benefit with gemcitabine as first-line therapy for patients with advanced pancreas cancer: a randomized trial. J Clin Oncol 1997;15:2403–13.
3. Louvet C, Labianca R, Hammel P, Lledo G, Zampino MG, Andre T, Zaniboni A, Ducreux M, Aitini E, Taieb J, Faroux R, Lepere C, et al. Gemcitabine in combination with oxaliplatin compared with gemcitabine alone in locally advanced or metastatic pancreatic cancer: results of a GERCOR and GISCAD phase III trial. J Clin Oncol 2005;23: 3509–16.
4. Bergman AM, Pinedo HM, Peters GJ. Determinants of resistance to 2′,2′-difluorodeoxycytidine (gemcitabine). Drug Resist Updat 2002;5:19–33.
5. Galmarini CM, Clarke ML, Falette N, Puisieux A, Mackey JR, Dumontet C. Expression of a non-functional p53 affects the sensitivity of cancer cells to gemcitabine. Int J Cancer 2002;97:439–45.
6. Shi X, Liu S, Kleeff J, Friess H, Buchler MW. Acquired resistance of pancreatic cancer cells towards 5-FU and gemcitabine is associated with altered expression of apoptosis-regulating genes. Oncology 2002;62: 354–62.
7. Duxbury MS, Ito H, Zinner MJ, Ashley SW, Whang EE. Inhibition of SRC tyrosine kinase impairs inherent and acquired gemcitabine resistance in human pancreatic adenocarcinoma cells. Clin Cancer Res 2004;10:2307–18.
8. Duxbury MS, Ito H, Benoit E, Zinner MJ, Ashley SW, Whang EE. RNA interference targeting focal adhesion kinase enhances pancreatic adenocarcinoma gemcitabine chemosensitivity. Biochem Biophys Res Commun 2003;311:786–92.
9. Akada M, Crnogorac-Jurcevic T, Lattimore S, Mahon P, Lopes R, Sunamura M, Matsuno S, Lemoine NR. Intrinsic chemoresistance to gemcitabine is associated with decreased expression of BNIP3 in pancreatic cancer. Clin Cancer Res 2005;11:3094–101.
10. Mackey JR, Mani RS, Selner M, Mowles D, Young JD, Belt JA, Crawford CR, Cass CE. Functional nucleoside transporters are required for gemcitabine influx and manifestation of toxicity in cancer cell lines. Cancer Res 1998;58:4349–57.
11. Rauchwerger DR, Firby PS, Hedley DW, Moore MJ. Equilibrative-sensitive nucleoside transporter and its role in gemcitabine sensitivity. Cancer Res 2000;60:6075–9.
12. Davidson JD, Ma L, Flagella M, Geeganage S, Gelbert LM, Slapak CA. An increase in the expression of ribonucleotide reductase large subunit 1 is associated with gemcitabine resistance in non-small cell lung cancer cell lines. Cancer Res 2004;64:3761–6.

13. Bergman AM, Eijk PP, Ruiz van Haperen VW, Smid K, Veerman G, Hubeek I, van den Ijssel P, Ylstra B, Peters GJ. In vivo induction of resistance to gemcitabine results in increased expression of ribonucleotide reductase subunit M1 as the major determinant. Cancer Res 2005;65:9510–16.
14. Dumontet C, Bauchu EC, Fabianowska K, Lepoivre M, Wyczechowska D, Bodin F, Rolland MO. Common resistance mechanisms to nucleoside analogues in variants of the human erythroleukemic line K562. Adv Exp Med Biol 1999;457:571–7.
15. Duxbury MS, Ito H, Zinner MJ, Ashley SW, Whang EE. RNA interference targeting the M2 subunit of ribonucleotide reductase enhances pancreatic adenocarcinoma chemosensitivity to gemcitabine. Oncogene 2004;23:1539–48.
16. Galmarini CM, Clarke ML, Jordheim L, Santos CL, Cros E, Mackey JR, Dumontet C. Resistance to gemcitabine in a human follicular lymphoma cell line is due to partial deletion of the deoxycytidine kinase gene. BMC Pharmacol 2004;4:8.
17. Eliopoulos N, Cournoyer D, Momparler RL. Drug resistance to 5-aza-2′-deoxycytidine, 2′,2′-difluorodeoxycytidine, and cytosine arabinoside conferred by retroviral-mediated transfer of human cytidine deaminase cDNA into murine cells. Cancer Chemother Pharmacol 1998;42: 373–8.
18. Hsu SI, Lothstein L, Horwitz SB. Differential overexpression of three mdr gene family members in multidrug-resistant J774.2 mouse cells. Evidence that distinct P-glycoprotein precursors are encoded by unique mdr genes. J Biol Chem 1989;264:12053–62.
19. Cole SP, Bhardwaj G, Gerlach JH, Mackie JE, Grant CE, Almquist KC, Stewart AJ, Kurz EU, Duncan AM, Deeley RG. Overexpression of a transporter gene in a multidrug-resistant human lung cancer cell line. Science 1992;258:1650–4.
20. Gatti L, Zunino F. Overview of tumor cell chemoresistance mechanisms. Methods Mol Med 2005;111:127–48.
21. Maehara S, Tanaka S, Shimada M, Shirabe K, Saito Y, Takahashi K, Maehara Y. Selenoprotein P, as a predictor for evaluating gemcitabine resistance in human pancreatic cancer cells. Int J Cancer 2004;112: 184–9.
22. Goan YG, Zhou B, Hu E, Mi S, Yen Y. Overexpression of ribonucleotide reductase as a mechanism of resistance to 2,2-difluorodeoxycytidine in the human KB cancer cell line. Cancer Res 1999;59:4204–7.
23. Mosmann T. Rapid colorimetric assay for cellular growth and survival: application to proliferation and cytotoxicity assays. J Immunol Methods 1983;65:55–63.
24. Braakhuis BJ, Ruiz van Haperen VW, Boven E, Veerman G, Peters GJ. Schedule-dependent antitumor effect of gemcitabine in in vivo model system. Semin Oncol 1995;22:42–6.
25. Tsujie M, Nakamori S, Okami J, Hayashi N, Hiraoka N, Nagano H, Dono K, Umeshita K, Sakon M, Monden M. Thiazolidinediones inhibit growth of gastrointestinal, biliary, and pancreatic adenocarcinoma cells through activation of the peroxisome proliferator-activated receptor gamma/retinoid X receptor alpha pathway. Exp Cell Res 2003; 289:143–51.
26. Murata S, Yoshiara T, Lim CR, Sugino M, Kogure M, Ohnuki T, Komurasaki T, Matsubara K. Psychophysiological stress-regulated gene expression in mice. FEBS Lett 2005;579:2137–42.
27. Takemasa I, Higuchi H, Yamamoto H, Sekimoto M, Tomita N, Nakamori S, Matoba R, Monden M, Matsubara K. Construction of preferential cDNA microarray specialized for human colorectal carcinoma: molecular sketch of colorectal cancer. Biochem Biophys Res Commun 2001;285:1244–9.
28. Finke J, Fritzen R, Ternes P, Lange W, Dolken G. An improved strategy and a useful housekeeping gene for RNA analysis from formalin-fixed, paraffin-embedded tissues by PCR. Biotechniques 1993;14: 448–53.
29. Miyamoto A, Nagano H, Sakon M, Fujiwara Y, Sugita Y, Eguchi H, Kondo M, Arai I, Morimoto O, Dono K, Umeshita K, Nakamori S, et al. Clinical application of quantitative analysis for detection of hematogenous spread of hepatocellular carcinoma by real-time PCR. Int J Oncol 2001;18:527–32.
30. Therasse P, Arbuck SG, Eisenhauer EA, Wanders J, Kaplan RS, Rubinstein L, Verweij J, Van Glabbeke M, van Oosterom AT, Christian MC, Gwyther SG. New guidelines to evaluate the response to treatment in solid tumors.European Organization for Research and Treatment of Cancer,National Cancer Institute of the United States,National Cancer Institute of Canada. J Natl Cancer Inst 2000;92:205–16.
31. Wright JA, Chan AK, Choy BK, Hurta RA, McClarty GA, Tagger AY. Regulation and drug resistance mechanisms of mammalian ribonucleotide reductase, and the significance to DNA synthesis. Biochem Cell Biol 1990;68:1364–71.
32. Hurta RA, Wright JA. Alterations in the activity and regulation of mammalian ribonucleotide reductase by chlorambucil, a DNA damaging agent. J Biol Chem 1992;267:7066–71.
33. Heinemann V, Xu YZ, Chubb S, Sen A, Hertel LW, Grindey GB, Plunkett W. Inhibition of ribonucleotide reduction in CCRF-CEM cells by 2′,2′-difluorodeoxycytidine. Mol Pharmacol 1990;38:567–72.
34. Jordan A, Reichard P. Ribonucleotide reductases. Annu Rev Biochem 1998;67:71–98.
35. Xue L, Zhou B, Liu X, Qiu W, Jin Z, Yen Y. Wild-type p53 regulates human ribonucleotide reductase by protein–protein interaction with p53R2 as well as hRRM2 subunits. Cancer Res 2003;63:980–6.
36. Eriksson S, Martin DW, Jr. Ribonucleotide reductase in cultured mouse lymphoma cells. Cell cycle-dependent variation in the activity of subunit protein M2. J Biol Chem 1981;256:9436–40.
37. Guittet O, Hakansson P, Voevodskaya N, Fridd S, Graslund A, Arakawa H, Nakamura Y, Thelander L. Mammalian p53R2 protein forms an active ribonucleotide reductase in vitro with the R1 protein, which is expressed both in resting cells in response to DNA damage and in proliferating cells. J Biol Chem 2001;276:40647–51.
38. Giroux V, Malicet C, Barthet M, Gironella M, Archange C, Dagorn JC, Vasseur S, Iovanna JL. p8 is a new target of gemcitabine in pancreatic cancer cells. Clin Cancer Res 2006;12:235–41.
39. Bepler G, Zheng Z, Gautam A, Sharma S, Cantor A, Sharma A, Cress WD, Kim YC, Rosell R, McBride C, Robinson L, Sommers E, et al. Ribonucleotide reductase M1 gene promoter activity, polymorphisms, population frequencies, and clinical relevance. Lung Cancer 2005;47: 183–92.
40. Jordheim LP, Guittet O, Lepoivre M, Galmarini CM, Dumontet C. Increased expression of the large subunit of ribonucleotide reductase is involved in resistance to gemcitabine in human mammary adenocarcinoma cells. Mol Cancer Ther 2005;4:1268–76.
41. Rosell R, Scagliotti G, Danenberg KD, Lord RV, Bepler G, Novello S, Cooc J, Crino L, Sanchez JJ, Taron M, Boni C, De Marinis F, et al. Transcripts in pretreatment biopsies from a three-arm randomized trial in metastatic non-small-cell lung cancer. Oncogene 2003;22:3548–53.
42. Rosell R, Danenberg KD, Alberola V, Bepler G, Sanchez JJ, Camps C, Provencio M, Isla D, Taron M, Diz P, Artal A. Ribonucleotide reductase messenger RNA expression and survival in gemcitabine/cisplatin-treated advanced non-small cell lung cancer patients. Clin Cancer Res 2004;10:1318–25.

Stronger growth-inhibitory effect of interferon (IFN)-ß compared to IFN-α is mediated by IFN signaling pathway in hepatocellular carcinoma cells

BAZARRAGCHAA DAMDINSUREN[1], HIROAKI NAGANO[1], HIROSHI WADA[1], MOTOI KONDO[1], HIDEO OTA[1], MASATO NAKAMURA[1], TAKEHIRO NODA[1], JAVZANDULAM NATSAG[2], HIROFUMI YAMAMOTO[1], YUICHIRO DOKI[1], KOJI UMESHITA[1], KEIZO DONO[1], SHOJI NAKAMORI[1], MASATO SAKON[1] and MORITO MONDEN[1]

Departments of [1]Surgery, and [2]Radiology, Graduate School of Medicine, Osaka University, Osaka, Japan

Received June 29, 2006; Accepted August 22, 2006

Abstract. Interferon (IFN) is a promising drug for prevention and treatment of hepatocellular carcinoma (HCC) in combination with chemotherapeutic agents. We previously reported that the spectra of antiproliferative activity and synergistic effect of IFN-ß when combined with anticancer drugs are more potent than those of IFN-α in HCC cells. However, the mechanism of the diverse antitumor effects of the IFNs is not understood yet. We studied the expression of IFN α receptor 2 (IFNAR2), STATs, and IFN-α, IFN-ß's growth-inhibitory effect, signal transduction and binding to IFNAR2 on three HCC cell lines and a tumor xenografted mouse model (12 animals/group). From the results, IFN-ß showed a significantly stronger growth-inhibitory effect than IFN-α on the HuH7 cell line (expressing low IFNAR2), however it was similarly high on PLC/PRF/5 and weak on HLE. In the nude mouse tumor xenograft model, IFN-ß injection significantly suppressed tumor volume relative to vehicle injection, while IFN-α showed weaker growth-inhibition. IFN signal transduction (phosphorylated-STAT1, 3) induced by IFN-ß was higher than that by IFN-α in HuH7 and tumor xenografts. Pretreatment of hepatoma cells with anti-IFNAR2 antibody blocked the IFN signaling, more for IFN-α. IFN-α's antiproliferative effect was reduced by the antibody in lower concentrations compared to that of IFN-ß. Taken together, the HCC cells that express low IFNAR2 and are resistant to IFN-α were sensitive to the growth-inhibitory effect of IFN-ß, which might be mediated by stronger IFN signal transduction and distinct binding to IFNAR compared to IFN-α.

Correspondence to: Dr Hiroaki Nagano, Department of Surgery, Graduate School of Medicine, Osaka University, 2-2 Yamadaoka E2, Suita, Osaka 565-0871, Japan
E-mail: hnagano@surg2.med.osaka-u.ac.jp

Key words: interferon-α/ß, interferon α receptor, STAT, antitumor effect, hepatocellular carcinoma

Introduction

Hepatocellular carcinoma (HCC) is one of the most common malignancies worldwide, with an estimated more than half a million new cases each year; most of which occur in Asia and Africa (1). The majority of patients are diagnosed at inoperable advanced stages and/or have recurrence or metastasis after therapy, and their prognoses remain extremely poor (2). Recent clinical trials on advanced HCC suggest that combination chemotherapies, especially 5-fluorouracil (5-FU) with interferon (IFN)-α may be effective (3-7). The response rate of these therapies ranged from 14 to 73% of selected patients with advanced HCC, unfortunately the remaining patients did not respond to the therapy and died within a few months. Therefore, more effective therapeutic strategies as well as alternative combination therapies are desirable in this field.

The actions of type I IFNs, which include IFN-α and -ß, are mediated by their interaction with a multisubunit cell-surface receptor, IFN α receptor (IFNAR)1 and IFNAR2 (8). From the IFNARs, IFNAR2 long-form (IFNAR2c) is suggested to be important for binding and signal transduction (9,10). After IFN binds to the receptors, IFNAR-associated tyrosine kinases (JAK) are activated, followed by phosphorylation of signal transducer and activator of transcription factor (STAT) 1, 2, and 3. Phosphorylated STATs (pSTAT) form hetero- or homo-dimers, and thus transfer into the nucleus leading to transcription of numerous IFN responsive genes that mediate antiviral, growth-inhibitory, apoptotic, anti-angiogenic and immunomodulatory responses (8).

The mechanisms of the antitumor effect of IFN-α and its combination with 5-FU against HCC have been studied previously. In *in vitro* studies, we showed that combination of IFN-α and 5-FU induces apoptosis through IFNAR2 and delays the progression of G1 to S-phase in an HCC cell line expressing IFNAR2 (11,12). Moreover, the spectra of the antiproliferative activity and synergistic effect of IFN-ß when

combined with anticancer drugs are more potent than those of IFN-α in HCC cells *in vitro* (13). However, the underlying mechanism of the diverse antitumor effect of IFN-α and IFN-ß is not understood yet. Therefore, the present study was conducted to confirm and to clarify the dissimilar antitumor effect of the IFNs *in vitro* and *in vivo*, concerning IFN signal transduction.

Materials and methods

Interferons and antibodies. Human purified natural IFN-α (OIF; Otsuka Pharmaceutical, Tokyo, Japan) and IFN-ß (IFN, Mochida; Mochida Pharmaceutical, Tokyo, Japan) were used in this study. The specific activities were 2.12×10^8 international units (IU)/mg and 3.7×10^8 IU/mg, respectively, and were used in the calculation of IFN concentrations in ng/ml for the experiments. Specific rabbit anti-human IFNAR2 (developed by Otsuka Pharmaceutical using recombinant human IFNAR2 as described in ref. 14), STAT1, pSTAT1 (Tyr701) (Cell Signaling Technology, Beverly, MA), STAT2, pSTAT2 (Tyr689) (Upstate Biotechnology, Lake Placid, NY), STAT3, pSTAT3 (Tyr705) (Cell Signaling Technology), actin (Sigma, St. Louis, MO), and donkey anti-rabbit coupled to horseradish peroxidase (Amersham Biosciences, Buckinghamshire, UK) antibodies were used.

Cell lines and culture. Human HCC cell lines, HuH7, PLC/PRF/5 and HLE, were purchased from the Japanese Cancer Research Resources Bank (Tokyo). The cells were maintained in Dulbecco's modified Eagle's medium supplemented with 10% fetal bovine serum (FBS), 100 U/ml penicillin and 100 µg/ml streptomycin at 37°C in a humidified incubator with 5% CO_2 in air.

For the study of phosphorylated STAT proteins, the cells were cultured in a medium containing 0.5% FBS for 2 days and then in FBS-free medium for 2 h. After that they were incubated in medium with or without a desired concentration of IFN-α or IFN-ß for selected time periods and harvested for Western blotting.

Growth inhibitory assay. Growth curves with IFNs were drawn as described previously (15). Briefly, the cells (2×10^4 cells/well for HuH7, 4×10^4 cells/well for PLC/PRF/5, 0.7×10^4 cells/well for HLE) were uniformly seeded in 12-well dishes, and from the next day they were treated with or without IFN-α or IFN-ß (2.5 ng/ml). On alternate days, the medium with IFNs was changed and the viable cells were counted using a Celltac semi-automatic analyzer (Nihon Kohden, Tokyo, Japan). The concentration of the IFNs applied here (equal to 500 IU/ml of IFN-α) was based on that used in our previous studies (11-13,16).

Nude mouse tumor xenograft model and IFN treatment. The HuH7 cells were injected subcutaneously (5×10^6 cells/animal) into the left flank of 4-week-old BALB/c nu/nu female mice (Japan Clea, Tokyo, Japan). Tumor size was measured twice a week using a caliper and tumor volume was calculated using the formula [tumor volume (mm^3) = (a^2 x b)/2], where a is the width and b is the length in mm. After attainment of tumor volume of ~50 mm^3 (10 days after injection), the mice were randomly assigned to one of three groups of 12 animals each, and IFN-α, IFN-ß (both 2×10^4 IU/animal) or PBS was injected subcutaneously three times a week. On the 21st treatment day the mice were sacrificed, and the tumors were harvested and stored at -80°C for further examination. The animal care was in accordance with the institutional guidelines, and the experiments were approved by the animal research committee of Osaka University.

Western blot analysis. The sub-confluent growing cells or tumor samples were washed with PBS (Sigma) and lysed in an ice-cold RIPA buffer with 1 mM sodium orthovanadate (15). Total protein concentration was determined using the Bradford protein assay (Bio-Rad, Hercules, CA) and Western blot analysis was performed as described in our previous studies (12,15). The antibodies were used at the following dilutions: 1:100 for detection of IFNAR2; 1:1000 for total-, phosphorylated-STAT1, 3 and actin; and 1:500 for STAT2. The expression of proteins was evaluated by measuring the optical densities of protein bands, using the National Institute of Health Image analysis software version 1.61 and the expression value was calculated relative to that of actin.

Neutralizing assays. For neutralizing assay of the anti-proliferative effect of IFNs, the cells were seeded to a 96-well microplate and, on the following day, escalating dilutions of anti-IFNAR2 antibody (1:500000-1:500, decided from experiments of cytotoxicity) were applied and, soon after (~30 min), either IFN-α or IFN-ß (until final concentration of 2.5 ng/ml) was added. The number of viable cells was measured 72 h later by MTT assay as described previously (13). The anti-IFNAR2 antibody does not cross-react with human IFN-α and IFN-ß by immunoblot (as described by the manufacturer).

To study the IFN signaling with anti-IFNAR2 antibody, the cells were cultured in medium (0.5% FBS) with or without the antibody (dilution 1:5000), and 24 h later they were treated with either IFN-α or IFN-ß (2.5 ng/ml) for 40 min, and thereafter harvested and probed to Western blotting.

Statistical analysis. Statistical analysis was performed using the Prism 4 program (GraphPad Software, San Diego, CA). Data from *in vitro* assays are expressed as mean ± SD from at least three independent experiments, and results from animal model experiments are shown as mean ± SEM. The Dunnett, and unpaired t-tests were used for analyses.

Results

IFN-ß exhibits a stronger growth-inhibitory effect than IFN-α on HuH7 cells in vitro and on nude mice tumor xenograft in vivo. To verify the growth-inhibitory effect of the IFNs in HCC cells, we drew the 8-day growth curves with or without 2.5 ng/ml of IFN-α or IFN-ß. As shown in Fig. 1, the IFNs exhibited diverse growth-inhibitory effects on the liver cells, i.e., strong growth-inhibition was observed on PLC/PRF/5 while IFNs did not show any effect on HLE (only with significant effect on the 8th day with IFN-ß). On the other hand, in the HuH7 cell line, IFN-ß significantly inhibited the cell growth while IFN-α did not; on the 8th day the growth

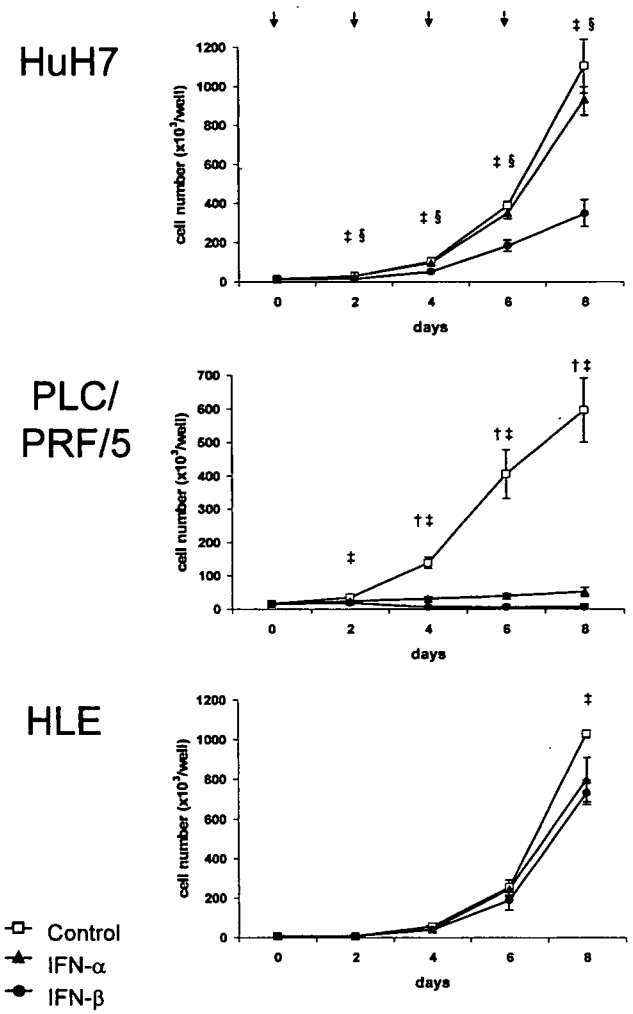

Figure 1. Growth-inhibitory effect of IFNs in HCC cell lines *in vitro*. Growth curves were drawn up to day 8 by counting viable cells treated or untreated with 2.5 ng/ml of IFN-α or IFN-β. Both IFNs exhibited strong cell growth suppression on the PLC/PRF/5 cell line. IFN-β resulted in significant growth inhibition of HuH7 cells compared to the control and IFN-α. HLE cells were resistant to both IFNs. Arrows denote change of fresh medium with the IFNs. †p<0.05, IFN-α vs vehicle; ‡p<0.05, IFN-β vs control (both by Dunnett's tests); §p<0.05, IFN-α vs IFN-β (by unpaired t-test).

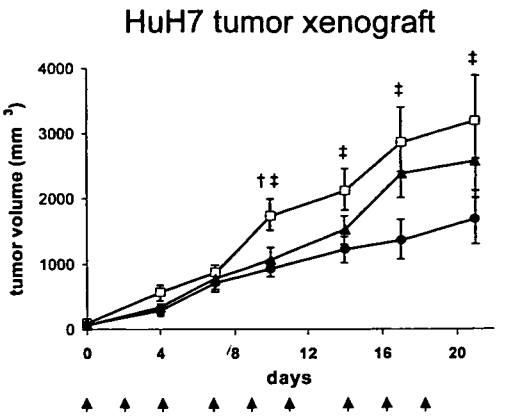

Figure 2. Effect of IFN-α and IFN-β on tumor growth *in vivo*. IFN-β therapy significantly inhibited the tumor growth from the 10th treatment day compared with the vehicle, while IFN-α exhibited less growth-inhibition (significant only on the 10th day). Arrows denote administration of the IFNs. †p<0.05, IFN-α vs vehicle; ‡p<0.05, IFN-β vs control (both by Dunnett's tests).

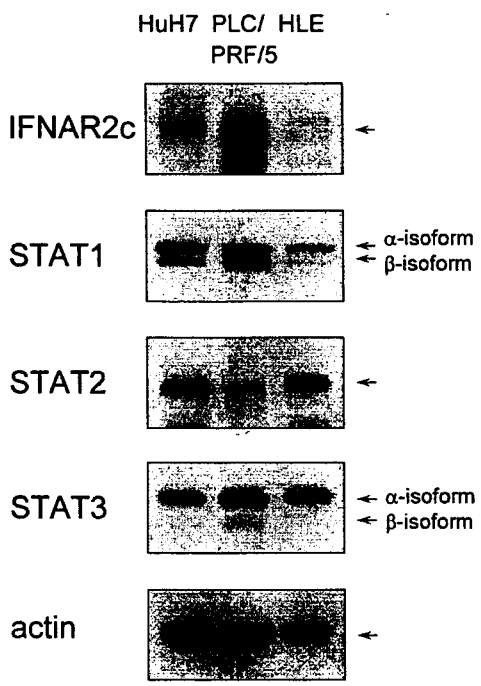

Figure 3. Expression of IFNAR2c and STATs in HCC cells. IFNAR2c was abundant in PLC/PRF/5, low in HuH7 and was lacking in HLE. STAT1 and 3 were expressed higher and STAT2 was less in PLC/PRF/5 compared to the other cells. Blots are representative of similar results of repeat experiments.

was inhibited by 68.5% with IFN-β ($p<0.01$ vs control, by Dunnett's test) and 15.5% with IFN-α ($p>0.05$). Moreover, the growth-inhibition was significantly stronger by IFN-β than by IFN-α from the 2nd day of treatment ($p<0.05$, by unpaired t-test).

To examine the effect of IFNs *in vivo*, we studied the growth of HuH7 tumor xenografts in nude mice with or without the IFN treatments ($2x10^4$ IU/animal thrice a week). As shown in Fig. 2, IFN-β therapy significantly inhibited tumor growth from the 10th day of treatment, compared with the vehicle ($p<0.05$ by unpaired t-test), while IFN-α treatment did not exhibit a significant growth-inhibitory effect (except on the 10th day). On the 21st post-treatment day, IFN-β resulted in a 47% decline of the tumor volume compared to that in the control animals ($p=0.03$), however IFN-α caused only 19% tumor growth regression ($p>0.05$). There was no difference in the body weights of animals in each group during the treatments (data not shown).

IFN-β-induced signaling is stronger than that of IFN-α in HuH7 in vitro and in vivo. At first, we examined the expression of IFNAR2c and STAT proteins in the cell lines. As shown in Fig. 3, the expression of IFNAR2c was abundant in IFN-sensitive PLC/PRF/5 cells, low in HuH7 and was lacking in HLE. STAT1 and 3 were expressed higher in PLC/PRF/5 than in other cells, however STAT2 was faint in PLC/PRF/5 while exhibiting clear bands in other cell lines.

To study IFN signal transduction, we treated the cells with different concentrations of the IFNs (0, 0.5, 2.5, 5.0 ng/ml) for 20 min and assessed the expression and activation of STAT proteins. The phosphorylations of STAT1 and 3 were activated

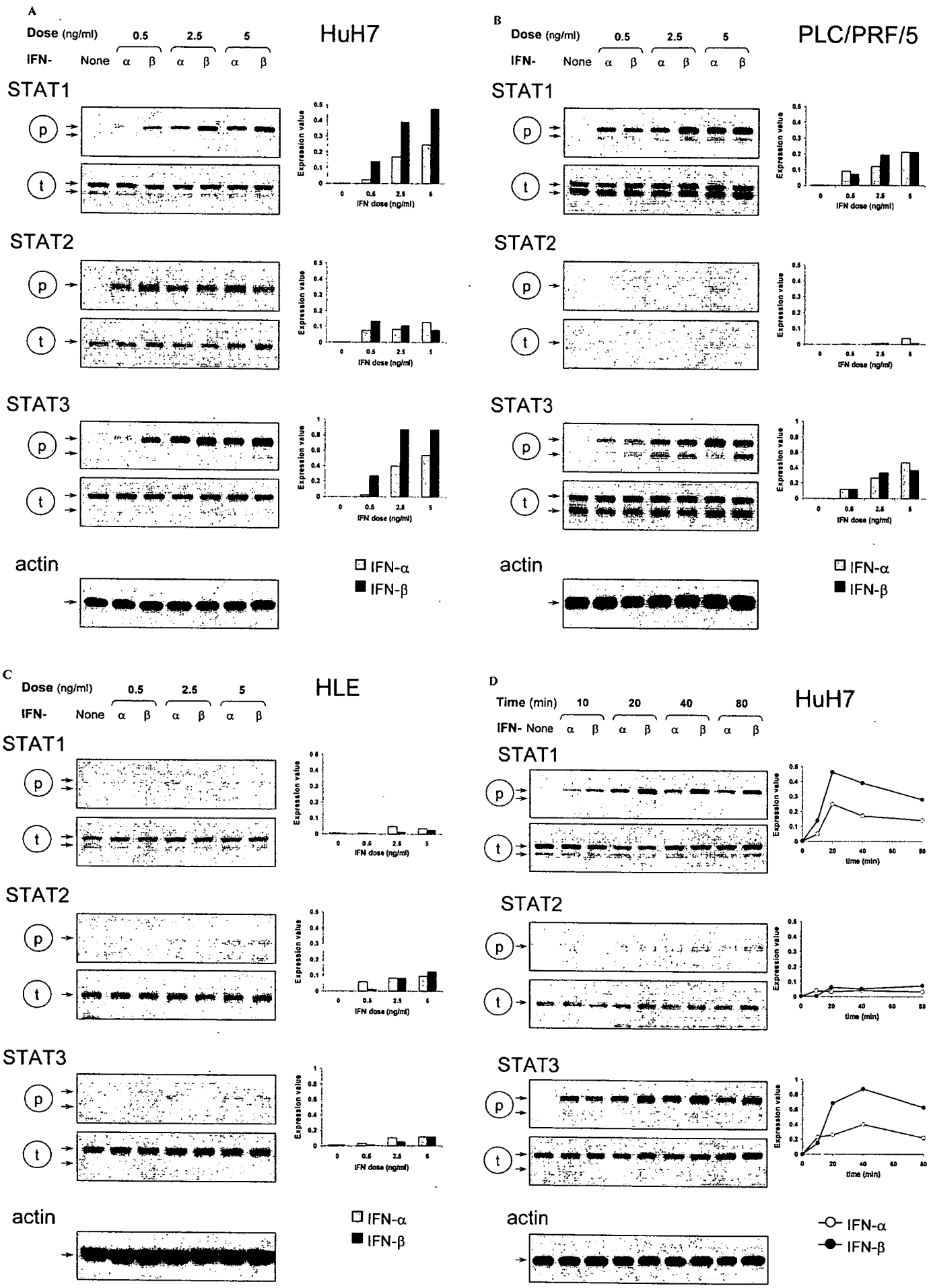
A
Dose (ng/ml) 0.5 2.5 5
IFN- None α β α β α β
HuH7
STAT1
STAT2
STAT3
actin
p
t
Expression value
IFN dose (ng/ml)
IFN-α
IFN-β
B
PLC/PRF/5
C
HLE
D
Time (min) 10 20 40 80
time (min)

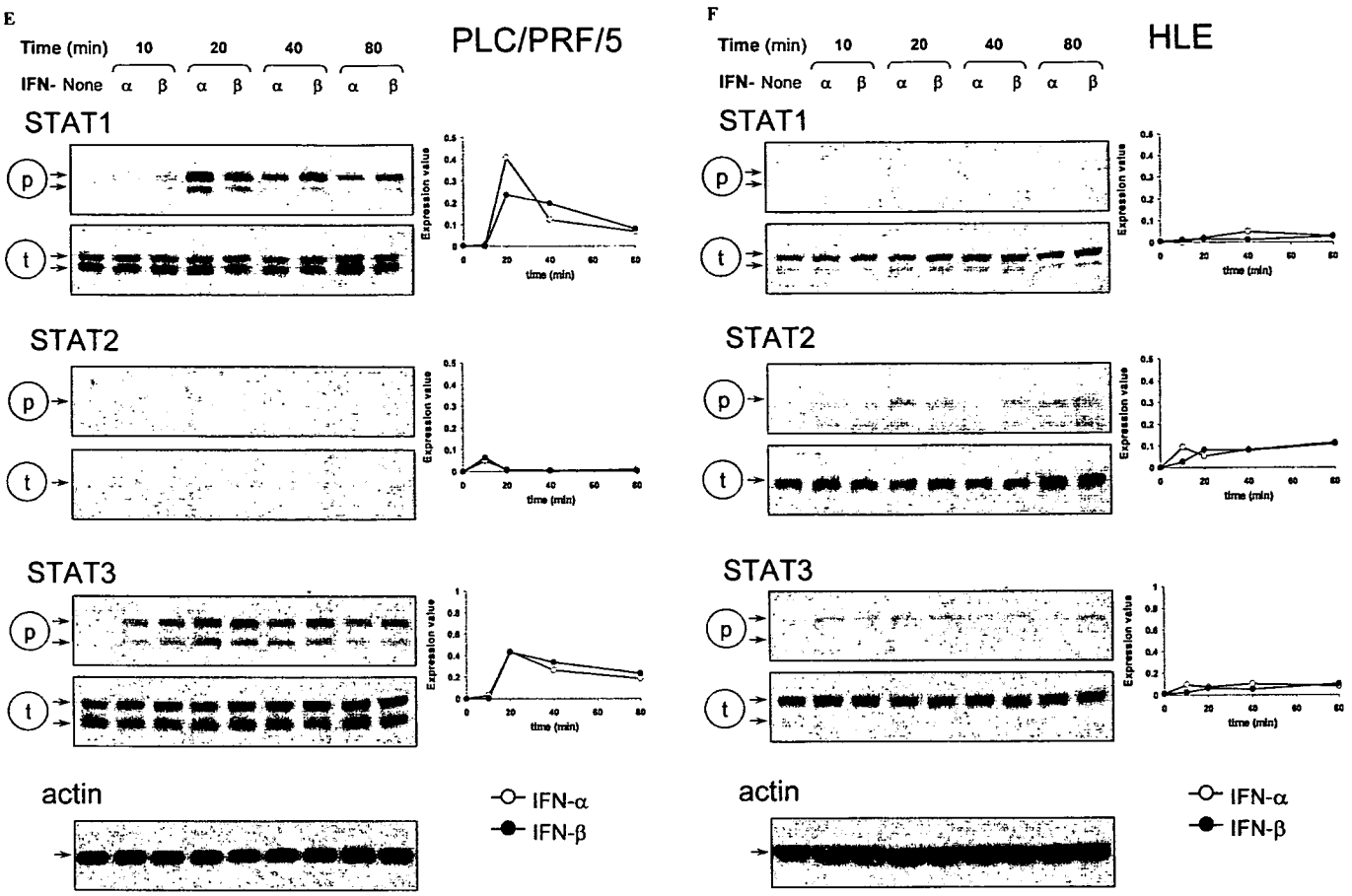

Figure 4. Activation of STATs by the IFNs in HCC cells. (A-C) Dose-dependency of induction of STATs. The cells were incubated with medium alone or diverse doses of the IFNs for equal amounts of time. The phosphorylation of STAT1 and 3 was dose-dependent from IFN concentration, and greater by IFN-ß induction than by IFN-α in HuH7 cells. However, pSTAT2 (A) and all total STATs were analogous. The signal transduction (pSTAT1, 3) induced by both IFNs was similarly intensive in PLC/PRF/5 (B) or faint in HLE cells (C). (D-F) Dynamics of STAT activation. The cells were treated for different amounts of time by either of the IFNs. In HuH7 cells, activation of STAT1 and 3 was noted for a longer time and at a higher level with IFN-ß than with IFN-α (D). p, phosphorylated; and t, total STAT. Graphs exhibit densities of respective pSTAT bands to actin. Data are representative of similar results of repeat experiments.

in a dose-dependent manner, while no such dose-dependent induction was observed for pSTAT2 (Fig. 4A-C). In the HuH7 cell line, which is more responsive to the growth-inhibitory effect of IFN-ß but not to that of IFN-α (Fig. 1), the phosphorylation of STAT1 and 3 was greater by IFN-ß than by IFN-α, respectively 5.8-, 2.3-, 1.9-fold and 10.6-, 2.2-, 1.6-fold higher in each IFN dose (Fig. 4A). The signal transduction induced by the IFNs was similarly high in PLC/PRF/5 (except expressing low pSTAT2), whereas it was equally faint in HLE cells (Fig. 4B and C).

When we examined the dynamics of STAT phosphorylation, the activation of STAT1 and 3 reached peaks within 20-40 min (Fig. 4D-F). In HuH7 cells, the higher pSTAT1 and 3 continued for a longer time with IFN-ß than with IFN-α (Fig. 4D). The expression of total STATs was not changed by the IFNs (corresponding lower blots).

Furthermore we examined the expression and activation of STATs in tumor xenograft samples. The IFN-ß-treated tumors showed greater induction of pSTAT3 than IFN-α-treated samples, while total STAT3 was analogous (Fig. 5). The activation of STAT1 and 2 was similarly faint in samples from both IFN-treated animals (data not shown).

Anti-IFNAR2 antibody suppresses differently the signaling and antiproliferative effects of IFN-α and IFN-ß. Because the signal transductions induced by the IFNs were different, and IFNAR2c is responsible for IFN signaling (9,10), we examined the IFN binding to the receptor using neutralizing antibody to the extracellular part of IFNAR2 on PLC/PRF/5 cells, which express abundant IFNAR2c (Fig. 2). Pretreatment of the cells with the antibody (dilution 1:5000) for 24 h blocked IFN signal transduction (pSTAT1) of both IFNs (Fig. 6A). The activation of STAT1 by IFN-α and -ß was decreased by 82.3 and 70.7% respectively. The expression of basic STAT1 did not change with addition of the antibody (data not shown).

When we examined the alteration of IFNs' anti-proliferative effect by anti-IFNAR2 antibody, it significantly reduced the effects in PLC/PRF/5 cells (Fig. 6B, asterisks denote significant differences compared to the IFN controls without the antibody by Dunnett's test). Furthermore, higher concentrations of the antibody were needed to suppress the effect of IFN-ß than of IFN-α (respectively dilutions 1:500 vs 1:5000). The effect of IFN-α disappeared with 1:5000 and 1:500 dilutions of the antibody ($p>0.05$ vs without IFN by Dunnett's test), while

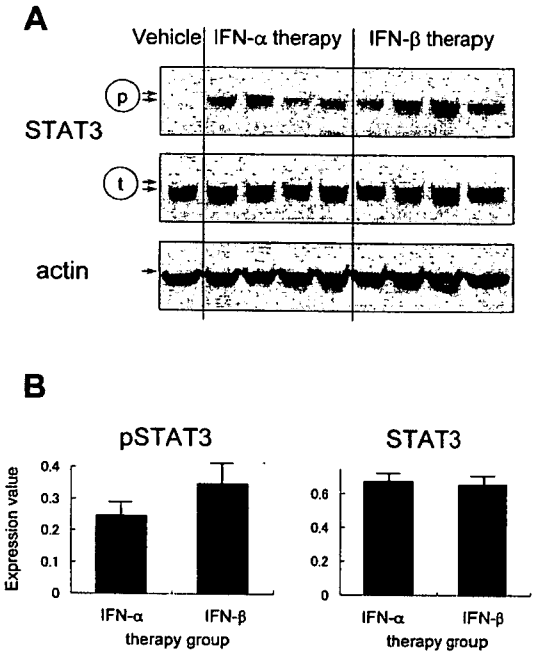

Figure 5. Expression and activation of STAT3 with the IFN treatments in tumor xenografts. One vehicle sample and four representative samples from each IFN-treated group are probed to Western blotting (A). IFN-ß-treated tumors showed greater induction of STAT3 phosphorylation than IFN-α treated tumors, while total STAT3 was analogous (B). p, phosphorylated; and t, total STAT.

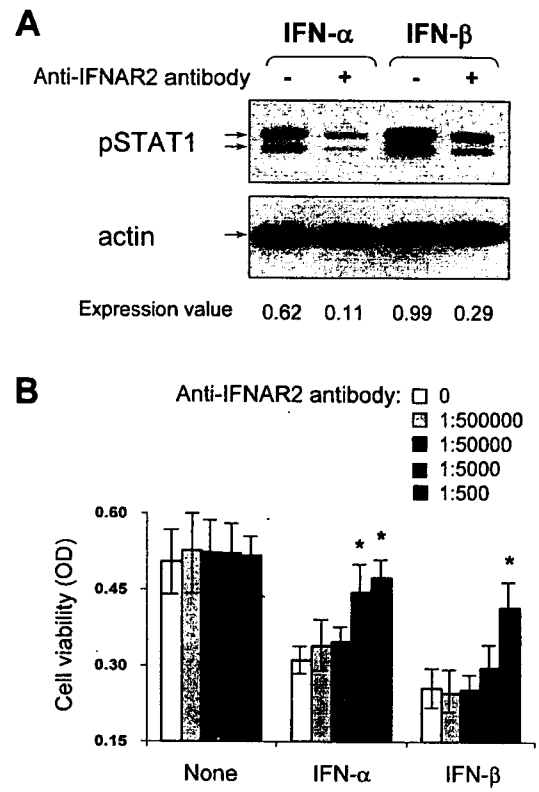

Figure 6. Neutralizing assays with anti-human IFNAR2 antibody on PLC/PRF/5 cells. (A) Blockade of IFN signaling by the antibody. The cells were incubated with or without 1:5000 diluted anti-IFNAR2 antibody for 24 h, then they were induced with 2.5 ng/ml either of IFN-α or IFN-ß. Induction of pSTAT1 was blocked for both IFNs, but less for IFN-ß, with the antibody. The expression value of each protein band was calculated relative to that of actin. Data are representative of similar results of repeat experiments. (B) The antiproliferative effect of the IFNs (2.5 ng/ml) was examined in the presence of serial dilutions of anti-IFNAR2 antibody as described in Materials and methods. The antibody significantly reduced the antiproliferative effect of IFNs (*$p<0.05$ vs control without the antibody by Dunnett's test). Suppression of the effects of IFN-ß required more antibody than that of IFN-α.

IFN-ß's effect was still observed with the same dilutions ($p<0.05$ vs without IFN).

Discussion

Herein we examined the growth-inhibitory action of IFN-α and IFN-ß on three HCC cell lines of different origin; PLC/PRF/5 cells were very sensitive and HLE cells were resistant to both IFNs. On the other hand, HuH7 cells, which showed resistance to the growth-inhibitory effect of IFN-α, were sensitive to IFN-ß (Fig. 1). IFN-ß also exhibited a stronger antitumor effect *in vivo* on xenografted HuH7 tumor model nude mice (Fig. 2). Consistently, the previous studies reported that IFN-ß has greater antitumor effects than IFN-α on melanoma, squamous carcinoma and breast cancer cells (17-19), however the mechanism of such distinct effects has not been studied.

We hypothesized that the investigation of IFN signal transduction could explain the differences in the IFNs' action, as well as the sensitivity of HCC cells to the IFNs. We found that the IFN-sensitive cells express higher IFNAR2, and subsequent phosphorylations of STAT1 and 3 by the IFNs were higher in these cells. Conversely, the resistant cells lack the receptor, and their IFN signaling was faint (Figs. 1, 3 and 4). The experiments on HuH7 cells, which express low IFNAR2, revealed the occurrence of stronger and persistent induction of pSTAT1 and 3 by IFN-ß compared to that induced by IFN-α. Still *in vivo* induction of pSTAT3 was more frequently observed in IFN-ß-treated tumors than in IFN-α-treated tumors. Therefore, the strong and continual signaling by IFN-ß in HuH7 cells may activate the transcription of various genes that result in a more potent antitumor effect. Previous studies reported that the IFNs produce variable induction of apoptosis and cell cycle inhibition in cancer cells (20-22).

Because the IFNs' signaling was different, we tried to investigate the binding of the IFNs to the receptors. For this purpose, we performed neutralizing experiments using an antibody binding to the extracellular part of IFNAR2. Our results on an HCC cell line with abundant receptor showed distinct suppression of the IFNs' effect and signal transduction when IFNAR2 is blocked (Fig. 6). This suggested that IFN-α and IFN-ß interact with IFNAR2 differently, although they share a common receptor. We also performed the neutralizing experiments on HuH7 cells, however the results were insignificant, perhaps because of less IFNAR2 expression in these cells and/or lower growth-inhibitory effect of the IFNs (data not shown). Differences in binding the IFNs to the IFN receptors were discussed previously; IFNAR2c subunit was distinctive for IFN-α and IFN-ß (23,24), or binding centers of the IFNs were different on the same IFNAR2 (25). Besides, the results may be related to the higher affinity binding of IFN-ß with the receptors than that of IFN-α (26).

Our findings further support these observations and were in agreement with suggestions that IFN-α's signaling might be transferred mainly through IFNAR2 (9,10), or blocking of IFNAR2 alone appears to be less sufficient for suppression of IFN-ß signal transduction.

From a clinical point of view, the usefulness of IFN-α monotherapy for HCC has been denied by randomized controlled trail study (27), and the promising combination therapy with subcutaneous IFN-α and intra-arterial 5-FU is less effective for patients with low IFNAR2 expression in tumor (6). Moreover, we found that 35% of the HCC patients exhibit no or faint expression of IFNAR2 (28). The correlation between clinical response of cancer patients to IFN therapy and *in vitro* susceptibility of malignant cells to IFN was reported previously (29). Therefore the present and our previous (13) *in vitro* and *in vivo* studies suggest that IFN-ß and/or its combination with anticancer drugs are promising for the treatment of human HCC with a possibility to improve the response rate, especially for patients with less IFNAR2.

In conclusion, our results suggest that the HCC cells that express low IFNAR2 and are resistant to IFN-α, might be sensitive to the growth-inhibitory effect of IFN-ß, which is mediated by stronger IFN signal transduction and has different binding to IFNARs compared to IFN-α.

Acknowledgments

This study was supported by a Grant-in-Aid for Scientific Research and for JSPS fellow provided by the Ministry of Education, Culture, Sports, Science and Technology, Japan. B.D. is a postdoctoral fellow supported by Japan Society for the Promotion of Science. The authors thank the Otsuka Pharmaceutical Co. for providing anti-human IFNAR polyclonal antibody.

References

1. El-Serag HB: Hepatocellular carcinoma: an epidemiologic view. J Clin Gastroenterol 35: S72-S78, 2002.
2. Llovet JM, Burroughs A and Bruix J: Hepatocellular carcinoma. Lancet 362: 1907-1917, 2003.
3. Sakon M, Nagano H, Dono K, Nakamori S, Umeshita K, Yamada A, Kawata S, Imai Y, Iijima S and Monden M: Combined intraarterial 5-fluorouracil and subcutaneous interferon-alpha therapy for advanced hepatocellular carcinoma with tumor thrombi in the major portal branches. Cancer 94: 435-442, 2002.
4. Patt YZ, Hassan MM, Lozano RD, Brown TD, Vauthey JN, Curley SA and Ellis LM: Phase II trial of systemic continuous fluorouracil and subcutaneous recombinant interferon Alfa-2b for treatment of hepatocellular carcinoma. J Clin Oncol 21: 421-427, 2003.
5. Nagano H, Sakon M, Eguchi H, Kondo M, Yamamoto T, Ota H, Nakamura M, Wada H, Damdinsuren B, Marubashi S, Miyamoto A, Takeda Y, Dono K, Umeshita K, Nakamori S and Monden M: Hepatic resection followed by IFN-alpha and 5-FU for advanced hepatocellular carcinoma with tumor thrombus in the major portal branch. Hepatogastroenterology (In press).
6. Ota H, Nagano H, Sakon M, Eguchi H, Kondo M, Yamamoto T, Nakamura M, Damdinsuren B, Wada H, Marubashi S, Miyamoto A, Dono K, Umeshita K, Nakamori S, Wakasa K and Monden M: Treatment of hepatocellular carcinoma with major portal vein thrombosis by combined therapy with subcutaneous interferon-alpha and intra-arterial 5-fluorouracil; role of type 1 interferon receptor expression. Br J Cancer 93: 557-564, 2005.
7. Obi S, Yoshida H, Toune R, Unuma T, Kanda M, Sato S, Tateishi R, Teratani T, Shiina S and Omata M: Combination therapy of intraarterial 5-fluorouracil and systemic interferon-alpha for advanced hepatocellular carcinoma with portal venous invasion. Cancer 106: 1990-1997, 2006.
8. Stark GR, Kerr IM, Williams BR, Silverman RH and Schreiber RD: How cells respond to interferons. Annu Rev Biochem 67: 227-264, 1998.
9. Domanski P, Witte M, Kellum M, Rubinstein M, Hackett R, Pitha P and Colamonici OR: Cloning and expression of a long form of the beta subunit of the interferon alpha beta receptor that is required for signaling. J Biol Chem 270: 21606-21611, 1995.
10. Kotenko SV, Izotova LS, Mirochnitchenko OV, Lee C and Pestka S: The intracellular domain of interferon-alpha receptor 2c (IFN-alphaR2c) chain is responsible for Stat activation. Proc Natl Acad Sci USA 96: 5007-5012, 1999.
11. Eguchi H, Nagano H, Yamamoto H, Miyamoto A, Kondo M, Dono K, Nakamori S, Umeshita K, Sakon M and Monden M: Augmentation of antitumor activity of 5-fluorouracil by interferon alpha is associated with up-regulation of p27Kip1 in human hepatocellular carcinoma cells. Clin Cancer Res 6: 2881-2890, 2000.
12. Kondo M, Nagano H, Wada H, Damdinsuren B, Yamamoto H, Hiraoka N, Eguchi H, Miyamoto A, Yamamoto T, Ota H, Nakamura M, Marubashi S, Dono K, Umeshita K, Nakamori S, Sakon M and Monden M: Combination of IFN-alpha and 5-fluorouracil induces apoptosis through IFN-alpha/beta receptor in human hepatocellular carcinoma cells. Clin Cancer Res 11: 1277-1286, 2005.
13. Damdinsuren B, Nagano H, Sakon M, Kondo M, Yamamoto T, Umeshita K, Dono K, Nakamori S and Monden M: Interferon-beta is more potent than interferon-alpha in inhibition of human hepatocellular carcinoma cell growth when used alone and in combination with anticancer drugs. Ann Surg Oncol 10: 1184-1190, 2003.
14. Novick D, Cohen B and Rubinstein M: The human interferon alpha/beta receptor: characterization and molecular cloning. Cell 77: 391-400, 1994.
15. Damdinsuren B, Nagano H, Kondo M, Natsag J, Hanada H, Nakamura M, Wada H, Kato H, Marubashi S, Miyamoto A, Takeda Y, Umeshita K, Dono K and Monden M: TGF-beta1-induced cell growth arrest and partial differentiation is related to the suppression of Id1 in human hepatoma cells. Oncol Rep 15: 401-408, 2006.
16. Yamamoto T, Nagano H, Sakon M, Wada H, Eguchi H, Kondo M, Damdinsuren B, Ota H, Nakamura M, Marubashi S, Miyamoto A, Dono K, Umeshita K, Nakamori S, Yagita H and Monden M: Partial contribution of tumor necrosis factor-related apoptosis-inducing ligand (TRAIL)/TRAIL receptor pathway to antitumor effects of interferon-alpha/5-fluorouracil against Hepatocellular Carcinoma. Clin Cancer Res 10: 7884-7895, 2004.
17. Horikoshi T, Fukuzawa K, Hanada N, Ezoe K, Eguchi H, Hamaoka S, Tsujiya H and Tsukamoto T: *In vitro* comparative study of the antitumor effects of human interferon-alpha, beta and gamma on the growth and invasive potential of human melanoma cells. J Dermatol 22: 631-636, 1995.
18. Giandomenico V, Vaccari G, Fiorucci G, Percario Z, Vannuchi S, Matarrese P, Malorni W, Romeo G and Affabris GR: Apoptosis and growth inhibition of squamous carcinoma cells treated with interferon-alpha, IFN-beta and retinoic acid are associated with induction of the cyclin-dependent kinase inhibitor p21. Eur Cytokine Netw 9: 619-631, 1998.
19. Coradini D, Biffi A, Pirronello E and Di Fronzo G: The effect of alpha-, beta- and gamma-interferon on the growth of breast cancer cell lines. Anticancer Res 14: 1779-1784, 1994.
20. Chawla-Sarkar M, Leaman DW and Borden EC: Preferential induction of apoptosis by interferon (IFN)-beta compared with IFN-alpha2: correlation with TRAIL/Apo2L induction in melanoma cell lines. Clin Cancer Res 7: 1821-1831, 2001.
21. Qin XQ, Runkel L, Deck C, De Dios C and Barsoum J: Interferon-beta induces S phase accumulation selectively in human transformed cells. J Interferon Cytokine Res 17: 355-367, 1997.
22. Sangfelt O and Strander H: Apoptosis and cell growth inhibition as antitumor effector functions of interferons. Med Oncol 18: 3-14, 2001.
23. Domanski P, Nadeau OW, Platanias LC, Fish E, Kellum M, Pitha P and Colamonici OR: Differential use of the betaL subunit of the type I interferon (IFN) receptor determines signaling specificity for IFNalpha2 and IFNbeta. J Biol Chem 273: 3144-3147, 1998.

24. Platanias LC, Uddin S, Domanski P and Colamonici OR: Differences in interferon alpha and beta signaling. Interferon beta selectively induces the interaction of the alpha and betaL subunits of the type I interferon receptor. J Biol Chem 271: 23630-23633, 1996.
25. Piehler J and Schreiber G: Mutational and structural analysis of the binding interface between type I interferons and their receptor Ifnar2. J Mol Biol 294: 223-237, 1999.
26. Russell-Harde D, Wagner TC, Perez HD and Croze E: Formation of a uniquely stable type I interferon receptor complex by interferon beta is dependent upon particular interactions between interferon beta and its receptor and independent of tyrosine phosphorylation. Biochem Biophys Res Commun 255: 539-544, 1999.
27. Llovet JM, Sala M, Castells L, Suarez Y, Vilana R, Bianchi L, Ayuso C, Vargas V, Rodes J and Bruix J: Randomized controlled trial of interferon treatment for advanced hepatocellular carcinoma. Hepatology 31: 54-58, 2000.
28. Kondo M, Nagano H, Sakon M, Yamamoto H, Morimoto O, Arai I, Miyamoto A, Eguchi H, Dono K, Nakamori S, Umeshita K, Wakasa K, Ohmoto Y and Monden M: Expression of interferon alpha/beta receptor in human hepatocellular carcinoma. Int J Oncol 17: 83-88, 2000.
29. Grander D, Oberg K, Lundqvist ML, Janson ET, Eriksson B and Einhorn S: Interferon-induced enhancement of 2',5'-oligoadenylate synthetase in mid-gut carcinoid tumours. Lancet 336: 337-340, 1990.

ELSEVIER

Journal of Hepatology 46 (2007) 77–88

Journal of Hepatology

www.elsevier.com/locate/jhep

Role of the Fas/FasL pathway in combination therapy with interferon-α and fluorouracil against hepatocellular carcinoma in vitro ☆,☆☆

Masato Nakamura, Hiroaki Nagano*, Masato Sakon, Tameyoshi Yamamoto, Hideo Ota, Hiroshi Wada, Bazarragchaa Damdinsuren, Takehiro Noda, Shigeru Marubashi, Atsushi Miyamoto, Yutaka Takeda, Koji Umeshita, Shoji Nakamori, Keizo Dono, Morito Monden

Department of Surgery, Graduate School of Medicine, Osaka University, Osaka, Japan

***Background/Aims*: Several studies have reported the efficacy of combination therapy of interferon (IFN) α and 5-fluorouracil (5-FU) for hepatocellular carcinoma (HCC). However, the mechanism underlying the clinical anti-tumor effects of this treatment is not well understood. The aim of this study was to determine the role of Fas/FasL signaling in the anti-tumor effect of this combination therapy.**

***Methods and Results*: We used six human hepatoma cell lines, three of which are known Fas-expressing cells. Growth of Fas-positive hepatoma cell lines was inhibited by an agonistic anti-Fas antibody in a dose-dependent manner, and these effects were enhanced by IFNα or 5-FU alone, but even more so by combination therapy using both agents. Annexin-V assay implicated apoptosis as the main mechanism underlying these growth inhibitory effects, although changes in Fas expression regulated by IFNα and/or 5-FU did not correlate with increased apoptosis. Caspase-3 activation was exclusively increased by IFNα/5-FU combination treatment, which was compatible with enhancement of the synergistic apoptotic effect, and other caspases and apoptotic factors (FLIP, BCL-xl, and Bax) were also regulated by IFNα/5-FU. ^{51}Cr-release assay revealed that pretreatment with IFN activated cytotoxicity of peripheral blood mononuclear cells (PBMCs) against HCC cells. The largest interaction was observed when both PBMC and HCC cells were pretreated with the combination of IFNα/5-FU. These cytotoxicities were markedly inhibited by a neutralizing anti-Fas antibody.**

***Conclusions*: Our results indicated that IFNα/5-FU combination treatment enhances the induction of apoptosis and the cytotoxic effect of PBMCs via the Fas/FasL pathway. The Fas/FasL pathway seems, at least in part, to contribute to the anti-tumor effects of IFNα/5-FU against HCCs.**

Keywords: **Hepatocellular carcinoma; Combination therapy; Interferon-α; 5-Fluorouracil; Apoptosis; Fas/FasL pathway; Caspase-3**

Received 21 February 2006; received in revised form 7 June 2006; accepted 5 July 2006; available online 25 September 2006

☆ This work was supported by a Grant-in-Aid for cancer research from the Ministry of Education, Culture, Sports, Science and Technology of Japan.

☆☆ The authors who have taken part in this study declared that they do not have a relationship with the manufacturers of the drugs involved either in the past or present and did not receive funding from the manufacturers to carry out their research.

* Corresponding author. Tel.: +81 6 6879 3251; fax: +81 6 6879 3259.
E-mail address: hnagano@surg2.med.osaka-u.ac.jp (H. Nagano).

1. Introduction

Hepatocellular carcinoma (HCC) is one of the most common solid tumors [1]. The prognosis for patients with HCC remains poor and most die within several months after diagnosis, particularly in advanced cases with tumor thrombosis in the major portal vein (Vp3-4) [2–4]. Chemotherapy is the traditional first choice

0168-8278/$32.00
doi:10.1016/j.jhep.2006.07.032

for the treatment of unresectable solid tumors; however, these drugs are not effective in promoting tumor regression and prolonging survival in HCC [5,6]. In addition, conventional therapeutic modalities such as transcatheter arterial embolization, radiofrequency ablation and microwave coagulation therapy are not recommended when portal vein tumor thrombosis (PVTT) is present because of low efficacy and potential complications [7,8]. Therefore, a new effective modality is needed to treat advanced HCC, especially in those cases with portal vein involvement.

Interferon (IFN) has a variety of biological properties including immunomodulation and anti-tumor activity. The anti-tumor effect of IFN against HCC was tested in several studies. From a randomized controlled trial, Llovet et al. [9] concluded that IFN used alone provides no clinical benefit for HCC patients with respect to tumor progression rate and survival. However, several other investigators reported a strong anti-tumor activity for IFN in HCC, when used in combination with some other chemotherapeutic agents. Urabe et al. [10] found that treatment with a combination of subcutaneous IFNα injection and intra-arterial infusion of 5-fluorouracil (FU), cisplatin and methotrexate for HCC with PVTT achieved a response rate of 46.7%. In addition, Patt et al. [11] reported that combination treatment with FU and IFN promoted anti-tumor has activity in HCC and could be tolerated even by cirrhotic patients. We also previously reported the beneficial results of subcutaneous IFNα injection and intra-arterial 5-FU infusion against HCC with PVTT [12–14]. This therapy showed an anti-tumor effect with a response rate approaching 50%, including several complete remissions of the tumor and prolonged survival without major adverse effects. From these results, we proposed that the combination chemotherapy of IFNα and 5-FU should become a standard therapy for advanced HCC.

We have already reported the synergistic effects of IFNα and 5-FU in influencing cell-cycle progression into the S phase via $p27^{Kip1}$, inducing apoptosis by downregulating Bcl-xl, and modulating the immune response via the TRAIL/TRAIL-receptor pathway [15–17]. The present study is an extension of this previous work, to investigate the role of the Fas/FasL pathway in the IFNα/5-FU treatment effect. Fas/FasL signaling participates in an apoptosis-inducing mechanism related to cytotoxic T Lymphocytes (CTL) and natural killer (NK) cells, which was implicated as a major pathway of T-cell-mediated cytotoxicity and a mediator of apoptosis via an IFN-stimulated gene [18]. In addition, we also investigated the mechanism underlying the apoptosis-enhancing effect of IFNα/5-FU that acts via the Fas/FasL pathway.

2. Materials and methods

2.1. Cells

Human HCC cell lines (HuH7, PLC/PRF/5, HLE, HLF and HepG2) were obtained from the Japan Cancer Research Resources Bank (JCRB) (Osaka, Japan) and the human HCC cell line, Hep3B, was obtained from the Institute of Development, Aging and Cancer, Tohoku University (Sendai, Japan). These cells were maintained in Dulbecco's modified Eagle's medium (DMEM) supplemented with 10% fetal bovine serum (FBS) and 1% penicillin at 37 °C in a humidified incubator with 5% CO_2 in air. A non-tumorigenic SV40-immortalized human liver epithelial cell line (THLE-2) was obtained from American Type Culture Collection (Manassas, VA). THLE-2 cells were maintained as an adherent monolayer in Bronchial epithelial medium (BEGM bullet kit, Combrex, NJ) from which remove the gentamicin/amphotericin and epinephrine and to which add extra 5 ng/ml EGF, 70 ng/ml phosphoethanolamine and 10% fetal bovine serum (FBS).

2.2. Reagents

Purified human IFNα was obtained from Otsuka Pharmaceutical Co. (Tokushima, Japan), and 5-FU was kindly provided by Kyowa Hakko Co. (Tokyo, Japan). Antibodies against Fas (UB-2, CH-11 and ZB4) were obtained from Medical and Biological Laboratories (Nagoya, Japan). Caspase-3-specific inhibitor (Z-DEVD-FMK), caspase-8-specific inhibitor (Z-IETD-FMK) and caspase-9-specific inhibitor (Z-LEHD-FMK) were purchased from Calbiochem (San Diego, CA).

2.3. Flow cytometric analysis of Fas expression

HCC cells were characterized for their surface expression of Fas receptors by flow cytometry. Cells (1×10^6) were incubated with 2.5 μg/ml of anti-Fas antibody (IgG, UB-2) for 30 min at 4 °C. After washing with PBS, the cells were analyzed on a FACScan (BD Transduction Laboratories, Lexington, KY), and data were processed using Cell Quest™ software (BD Transduction Laboratories).

2.4. Cell growth assay

Cell growth was assessed by the 3-(4-,5-dimethylthiazol-2-yl)-2,5-diphenyl tetrazolium bromide (MTT) assay. Briefly, 3×10^4 cells were seeded on a 96-well plate in 100 μl of medium and left overnight to adhere. Several concentrations of the test drugs in 100 μl volumes were added, and the cells were incubated for 48 h. After treatment, 10 μl of MTT solution was added to each well and incubated for another 4 h at 37 °C. Then 100 μl of acid–isopropanol was added, and after 24 h at 4 °C, reduced MTT was measured spectrophotometrically in a dual-beam microtiter plate reader at 570 nm with a 650 nm reference.

2.5. Flow cytometric analysis of annexin V-FITC binding

The binding of annexin V-FITC was used as a sensitive method for measuring apoptosis, according to a modification of a previously described method [19]. Briefly, after treatment with IFNα/5-FU and/or anti-Fas antibody CH-11, the cultured cells (1×10^6) were incubated with binding buffer (10 mM Hepes, 140 mM NaCl and 2.5 mM $CaCl_2$, pH 7.4) containing saturating concentrations of annexin V-FITC (BioVision Research Products, Mountain View, CA) and propidium iodide (PI) for 15 min at room temperature. After incubation, the cells were pelleted and analyzed on a FACScan (BD), and data were processed using Cell Quest™ software (BD).

2.6. Caspase activity

After treatment with the test drugs and/or anti-Fas antibody, cytosolic extracts were prepared using lysis buffer. The caspase activity in the cell cytosol was measured using a Caspase Colorimetric Protease Assay Kit (MBL) as per the instructions provided by the manufacturer. This assay is based on the spectrophotometric detection of the chromophore, *p*-nitroanilide after cleavage from the labeled substrate. Caspase-3, -8 and -9 assay kits were used in this study.

2.7. Real-time PCR

The LightCycler PCR and detection system (Roche Diagnostics, Mannheim, Germany) was used for amplification and quantification. For detection of glyceraldehyde-3-phosphate dehydrogenase (GAPDH) and the amplification products of some apoptotic factors, the LightCycler DNA Master SYBR Green I (Boehringer Mannheim, Mannheim, Germany) was used. Real-time PCRs were performed in a sample mixture containing each primer (final concentration, 0.2 μM), 1× LC-DNA Master SYBR Green I, 4 mM of $MgCl_2$, and 2 μl of cDNA as a template using the following primers: human GAPDH (forward: 5′-CAACTACATGGTTTACATGTTC-3′, reverse: 5′-GCCAGTGGACTCCACGAC-3′); Bcl-xl (forward: 5′-GTAAACTGGGGTCGCATTGT-3′, reverse: 5′-TGGATCCAAGGCTCTAG GTG-3′), and Bax (forward: 5′-CCAGCTGCCTTG GACTGT-3′, reverse: 5′-ACCCCCTCAAGACCACTCTT-3′) yielding products of 182, 146 and 135 bp, respectively [20]. The GAPDH PCR cycle conditions were set up as follows: one cycle of 95 °C for 10 min, followed by 40 cycles of 95 °C for 15 s, 55 °C for 10 s and 72 °C for 20 s. Fluorescence was acquired at the end of every 72 °C extension phase. The annealing temperatures for Bcl-xl and Bax were 60 and 61 °C, respectively. Quantitative analysis of data was performed using the LightCycler™ analysis software (Roche Diagnostics).

2.8. Western blot analysis

The sub-confluent growing cells were washed with PBS (Sigma) and lysed in an ice-cold RIPA buffer [25 mM Tris (pH 7.5), 50 mM NaCl, 0.5% sodium deoxycholate, 2% Nonidet P-40, 0.2% SDS, 1 mM phenylmethylsulfonyl fluoride and 500 KIE/ml "Trasylol"® proteinase inhibitor (Bayer Leverkusen, Germany)]. Total protein concentration was determined using the Bradford protein assay (Bio-Rad, Hercules, CA) and Western blot analysis was performed as described in our previous study [17]. The antibodies were used in dilutions of 1:100 for FLIPS/L (sc-5276; Santa Cruz Biotechnology, Santa Cruz, CA), 1:1000 for actin (A-2066; Sigma), and 1:2000 for secondary donkey anti-rabbit (NA934V; Amersham Biosciences, Buckinghamshire, UK) antibodies. The expression of proteins was evaluated by measuring the optical densities of protein bands, using the National Institute of Health Image analysis software version 1.61 and the expression value was calculated relative to that of actin.

2.9. Cytotoxicity assay

Target cells (1×10^6) were labeled with 40 μCi $Na^{51}CrO_4$ for 45 min at 37 °C. ^{51}Cr-labeled target cells (1×10^4) and effector cells (peripheral blood mononuclear cells, PBMCs) were mixed in U-bottomed wells of a 96-well microplate at the indicated *E/T* ratios. After 8 h of incubation, the cell-free supernatants were collected and counted on a gamma counter. The percent-specific cytotoxicity was calculated using the formula: [100 × (experimental release − spontaneous release)/(total release − spontaneous release)]. Total or spontaneous release was determined in the presence of 1% NP-40 or medium alone. For blocking, anti-Fas mAb ZB-4 was added at a final concentration of 500 ng/ml before the cytotoxicity assay for 1 h in accordance with the manufacturer's instructions.

2.10. Magnetic sorting

PBMCs obtained from a healthy volunteer were prepared by Ficoll–Hypaque centrifugation. $CD4^+$ T cells, $CD8^+$ T cells, and $CD4^-CD8^-$ cells were isolated from PBMCs by using anti-CD4 and anti-CD8 immunomagnetic beads and a Magnetic Cell Sorter (Miltenyi Biotec, Bergisch Gladbach, Germany). The purity of each subset was estimated at >95% by flow cytometry.

2.11. TUNEL assay

To detect apoptosis, we used the terminal deoxynucleotidyl transferase-mediated dUTP nick end-labeling (TUNEL) method, using the Apop Tag in situ apoptosis detection Kit (Chemicon International, Inc., Temecula, CA) as described previously [17]. This method can detect fragmented DNA ends of apoptotic cells. Briefly, the paraffin-embedded sections were deparaffinized in xylene and rehydrated in a graded series of ethanol baths. The sections were treated with 20 μg/ml of proteinase K in distilled water for 10 min at room temperature. The adherent cultured THLE-2 cells were fixed in 1% paraformaldehyde for 10 min. To block endogenous peroxidase, the slides were incubated in methanol containing 0.3% hydrogen peroxide for 20 min. The remaining procedures were performed according to the instructions provided by the manufacturer. For quantification of apoptosis, five microscopic fields were randomly selected at high power magnification (200×) and the average counts of TUNEL-positive cells were calculated.

2.12. Statistical analysis

Statistical analysis was performed using the StatView J-5.0 program (Abacus Concepts, Inc., Berkeley, CA). Data are expressed as means ± SD. Differences between groups were examined for statistical significance using the Dunnett method and Student's *t*-test. $P < 0.05$ denotes a statistically significant difference.

3. Results

3.1. Fas expression in human hepatoma cell lines

Flow cytometry using an anti-Fas antibody (UB-2) revealed expression of Fas receptor on the cell surface in three of the six cell lines (HLE, HLF and HepG2), but not on HuH7, PLC/PRF/5 and Hep3B (Fig. 1).

3.2. Response to agonistic anti-Fas antibody with dose escalation

We confirmed the response described above using the agonistic anti-Fas monoclonal antibody, CH-11, which is used widely to replace FasL in vitro. The 48-h MTT assay showed that CH-11 treatment inhibited the growth of three Fas-positive hepatoma cell lines (HLE, HLF and HepG2) in a dose-dependent manner. In contrast, no Fas-negative cell lines (HuH7, PLC/PRF/5 and Hep3B) were growth-responsive to CH-11 (Fig. 2a). Dose dependency of IFNα and 5-FU was examined with various CH-11 concentrations. This effect was synergistic and observed in the combination of CH-11 and 5-FU in the doses of 0–0.5 μg/ml of 5-FU. There was seen little difference between 0.5 and 1 μg/ml of 5-FU (Fig. 2b).

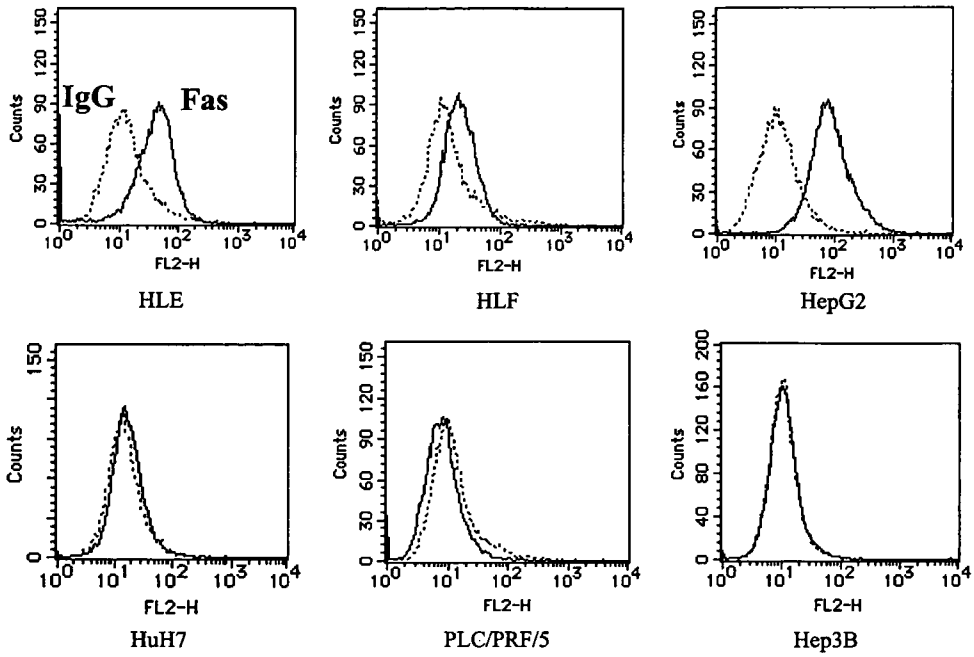

Fig. 1. Fas expression in six hepatoma cell lines assessed using flow cytometry with an anti-human Fas antibody (IgG, clone UB2). Histogram with dotted line represents cells stained with secondary antibody alone; histogram with solid line is those cells stained with anti-Fas antibody. Fas was expressed on the surface of three of the six cell lines (HLE, HLF and HepG2). All experiments were performed three times independently.

3.3. Influence of IFNα and/or 5-FU on apoptosis induced by agonistic anti-Fas antibody

We next evaluated the effects of IFNα, 5-FU and combination treatments on growth inhibition induced by CH-11 using the MTT assay. In Fas-expressing cell lines, the inhibitory effect of CH-11 was enhanced with IFNα or 5-FU alone, but the maximum effect was observed with a combination treatment of both agents (Fig. 3a). In the HepG2 cells, the anti-proliferating effect of CH-11 alone was 26.7 ± 1.8%, and the effect of either IFNα or 5-FU used alone was 18.0 ± 4.7%, which did represent a significant enhancement. However, the combination treatment (CH-11 + IFNα/5-FU) yielded a markedly increased effect of 83.8 ± 6.3% ($P = 0.01$). Without CH-11, none of the agents, whether used alone or in combination, had any anti-proliferative effects. Similar results were obtained in the other Fas-positive cell lines, HLE and HLF.

To confirm these results, we performed an annexin-V assay to detect Fas-mediated apoptosis. Results with the HepG2 cells were comparable with those from the MTT assay (Fig. 3b, Table 1), in that an increase in apoptotic cell numbers induced by CH-11 was found with stimulation by IFNα alone, 5-FU alone, and particularly strongly with the combination treatment. In contrast, the effects of CH-11 and the influence of IFNα/5-FU were not observed with the three Fas-negative cell lines (HuH7, PLC/PRF/5 and Hep3B) in both the MTT and annexin-V assay (Fig. 3a; MTT assay, data not shown; annexin-V assay).

3.4. Regulation of Fas expression by IFNα and/or 5-FU

To investigate the mechanism underlying the upregulation of Fas-mediated apoptosis, we analyzed the relationship between the change in Fas expression and the regulation of apoptosis. Out of the six cell lines, 5-FU increased Fas expression in the HepG2 cells only, while IFNα also increased Fas in the HuH7 and PLC/PRF/5 cells (Fig. 4). No additional effects were seen with the combination of IFNα and 5-FU compared with each drug used alone. In the other three hepatoma cell lines (HLE, HLF and Hep3B), neither IFNα nor 5-FU affected the level of cell surface Fas.

3.5. Caspase activation after stimulation with agonistic anti-Fas antibody and/or IFNα/5-FU

Results indicated that the change in Fas expression seen in this study would not be related to the CH-11 and IFNα/5-FU-mediated effects on apoptosis. Therefore, we next tested for variations in caspase activity in the HepG2 cells, as the representative Fas-positive cell line, using a caspase colorimetric protease assay kit (Fig. 5a). Caspase-3 activity (downstream of caspase cascades) was increased after 12 h of CH-11 stimulation. IFNα and 5-FU alone enhanced this upregulation, with the combination treatment having a further effect (Fig. 5a); 5-FU alone, IFNα alone and combination therapy did not affect caspase-3 activity without CH-11. Caspase-8 activity also

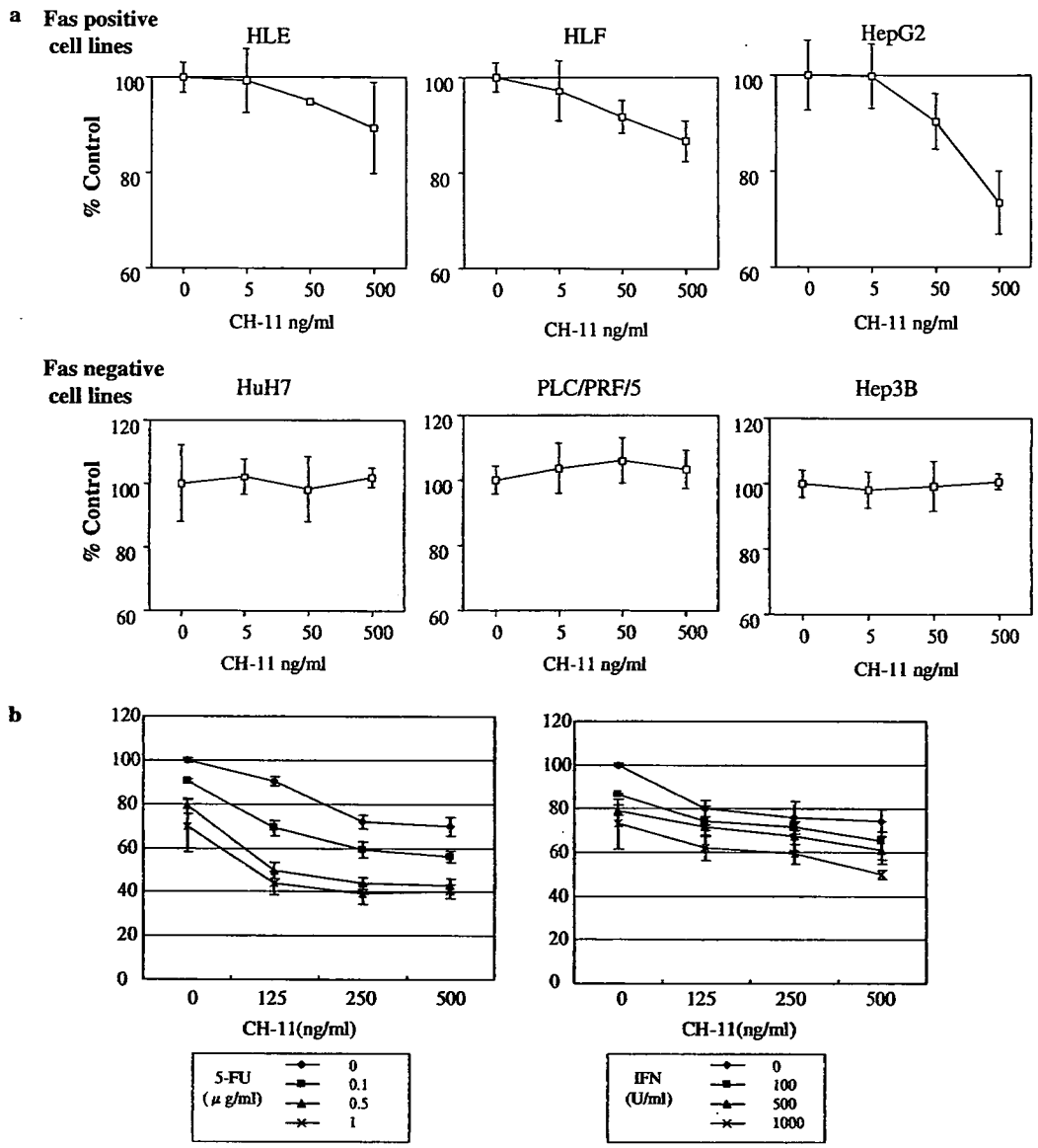

Fig. 2. Susceptibility of six hepatoma cell lines to agonistic anti-Fas monoclonal antibody CH-11-mediated apoptosis was measured by MTT assay. (a) Each cell line was incubated with CH-11 at various concentrations for 48 h. Three Fas-positive cell lines (HLE, HLF and HepG2) were naive to CH-11 in a dose–response manner. Fas-negative cell lines (HuH7, PLC/PRF/5 and Hep3B) were resistant to Fas-mediated apoptosis. (b) Dose dependency of combination treatment was examined. CH-11 and 5-FU or IFNα were added to HepG2 cells with indicated doses. Results are expressed as percent of cell growth of each untreated cell. Data represent means ± SD of at least triplicate samples. Similar results were observed in three independent experiments.

increased with CH-11 stimulation compared with the control and further increased with CH-11 + IFNα/5-FU; there was no significant difference between stimulation of CH-11 + IFNα and the combination. On the other hand, caspase-9 activity showed a different tendency from the data for caspase-3 and -8. Stimulation with CH-11+5-FU or CH-11 + IFNα/5-FU slightly increased the caspase-9 activity, but the effects were much less pronounced than for caspase-3 and caspase-8, and they were not significant (Fig. 5a). To confirm the significance of caspase activities in the apoptotic effect in Fas/FasL system, MTT assay using specific caspase inhibitors was performed. All specific caspase inhibitors blocked the apoptotic effect of CH-11 with IFNα/5-FU totally or partially in the dose-dependent manner (data not shown). Caspase-3-specific inhibitor (Z-DEVD-FMK) and caspase-8-specific inhibitor (Z-IETD-FMK) almost completely blocked CH-11 induced apoptosis enhanced by IFNα/5-FU (Fig. 5b). Caspase-9-specific inhibitor (Z-LEHD-FMK) showed only partial blocking effect. These results were compatible to the results of caspase assay (Fig. 5a). Colorimetric caspase assay using specific caspase inhibitors showed Z-DEVD-FMK blocked caspase-3 activation induced by CH-11 and IFNα/5-FU (Fig. 5c).

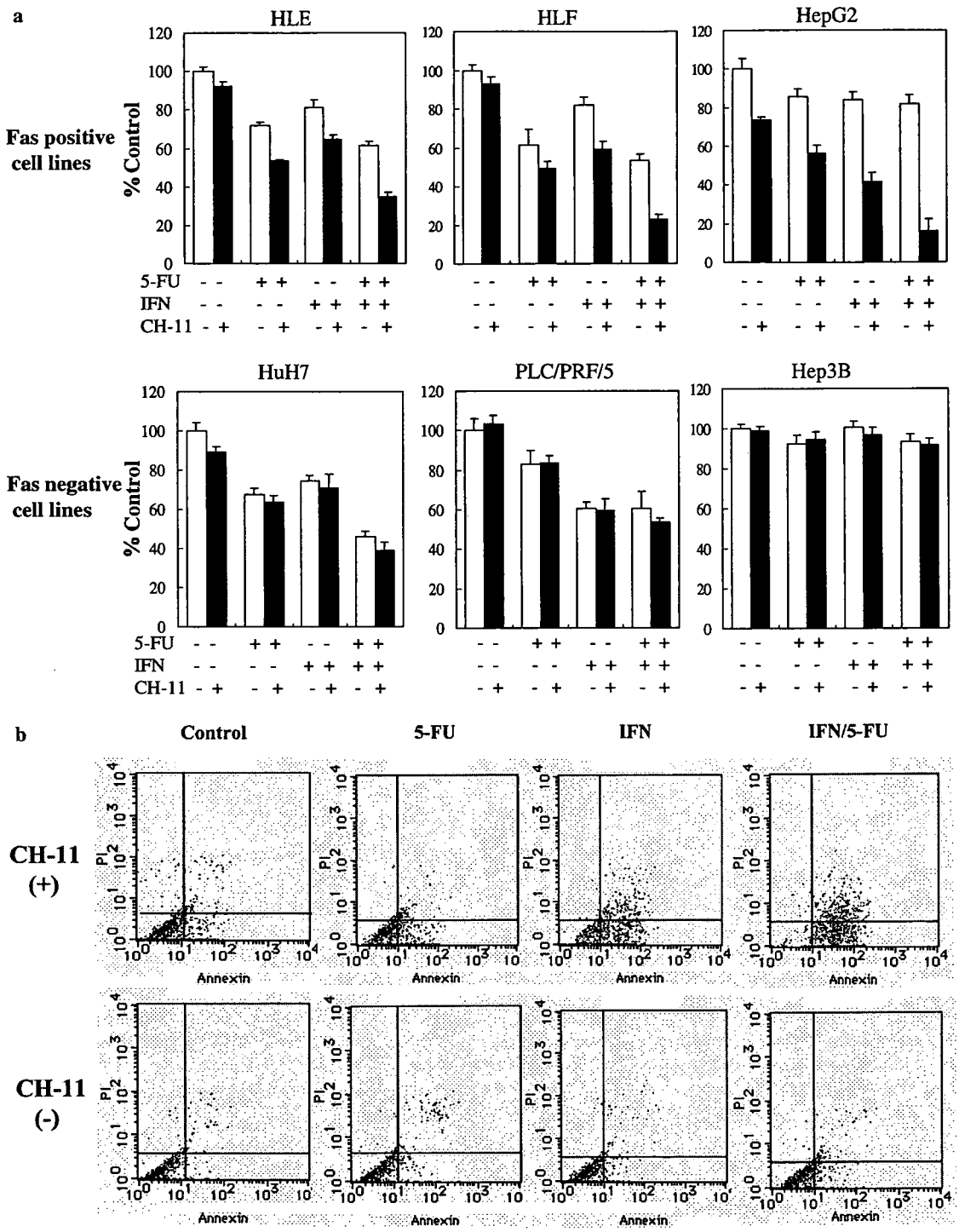

Fig. 3. (a) Effects of IFNα and/or 5-FU on Fas-mediated apoptosis in six hepatoma cell lines measured by MTT assay. All cells were incubated with IFNα (500 U/ml) and/or 5-FU (0.5 μg/ml) and with agonistic anti-Fas monoclonal antibody CH-11 (500 ng/ml) (□) or without CH-11 (■) for 48 h. The susceptibility of Fas-positive hepatoma cells to Fas-mediated apoptosis was significantly enhanced by IFNα or 5-FU alone, and further so in the combination treatment. Results were expressed as percent of cell viability of untreated cells. Data represent means ± SD values of at least triplicate samples. Similar results were observed in three independent experiments. (b) Apoptotic cells were determined using the annexin-V assay (HepG2). [This figure appears in colour on the web.]

3.6. Regulation of FLIP

Several factors involved in apoptosis were next examined at the mRNA expression level. The expression of FLIP (FLICE/caspase-8 inhibitory protein), which is an inhibitor of caspase-8 [21,22], was markedly decreased by treatment with IFNα or 5-FU, as shown by the FLIP/GAPDH ratio, compared with untreated

Table 1
Comparison of results of MTT and annexin-V assays

	Cell toxicity (%)	Annexin (+) cells (%)
Control	0.0	5.8
5-FU	14.4	9.5
IFN	16.2	10.0
IFN + 5FU	18.0	19.7
CH-11	26.7	27.8
CH-11 + 5FU	43.8	37.6
CH-11 + IFN	58.0	62.4
CH-11 + IFN + 5FU	83.8	93.5

The two independent assays showed similar tendency. Annexin-V assay indicated that the growth inhibition effect noted in MTT assay was caused by apoptosis.

cells with the combination treatment again providing the most significant decrease (Fig. 6a). Western blot analysis was performed to examine the change of FLIP at protein level. Expression of FLIP long was decreased by the combination treatment (Fig. 6b).

3.7. Regulation of apoptotic factors

Caspase-9 acts through mitochondria and is regulated by certain apoptotic factors [23]. Although the levels of caspase-9 were not increased, we checked the expression of the apoptotic factors Bax and Bcl-xl (Fig. 6c). The IFNα/5-FU combination significantly increased Bax expression, although the effect was not dramatic. Each of the above treatments in turn reduced Bcl-xl expression, although in this case the IFNα/5-FU combination produced no enhancement.

3.8. Involvement of the Fas/FasL pathway in IFNα/5-FU-induced PBMC cytotoxicity against HCC cells

We performed ^{51}Cr-release assay to evaluate the interaction between PBMC and hepatoma cell lines via the Fas/FasL pathway by which IFNα/5-FU appear to exert their influence (Fig. 7). In the Fas-positive HepG2 cells, we first established the optimal *E/T* ratio, which is directly proportional to the increase in released ^{51}Cr (Fig. 7a). The blocking effect of neutralizing anti-Fas antibody, ZB-4, is shown in Fig. 7b. Based on these data, an *E/T* ratio of 20 was chosen, to produce the most distinct difference in the presence and absence of ZB4 (Fig. 7c). Fig. 7c shows that IFNα increased the released ^{51}Cr and that this enhanced cytotoxicity was blocked by ZB4. Next, we tried to identify the main proponent of the cytotoxic effect using a magnetic sorting technique. $CD4^+$ cells, $CD8^+$ cells, and $CD4^-CD8^-$ cells were isolated from PBMCs and used as effecter cells in the ^{51}Cr-release assay after pretreatment with IFNα and/or 5-FU (Fig. 7d). The HepG2 target cells received no pretreatment. The results show that the $CD4^-CD8^-$ cells were the most cytotoxic and that IFNα enhanced this effect more than 5-fold. This IFNα-induced cytotoxicity was markedly inhibited by ZB4. Lastly, we pretreated both effecter and target cells with IFNα/5-FU

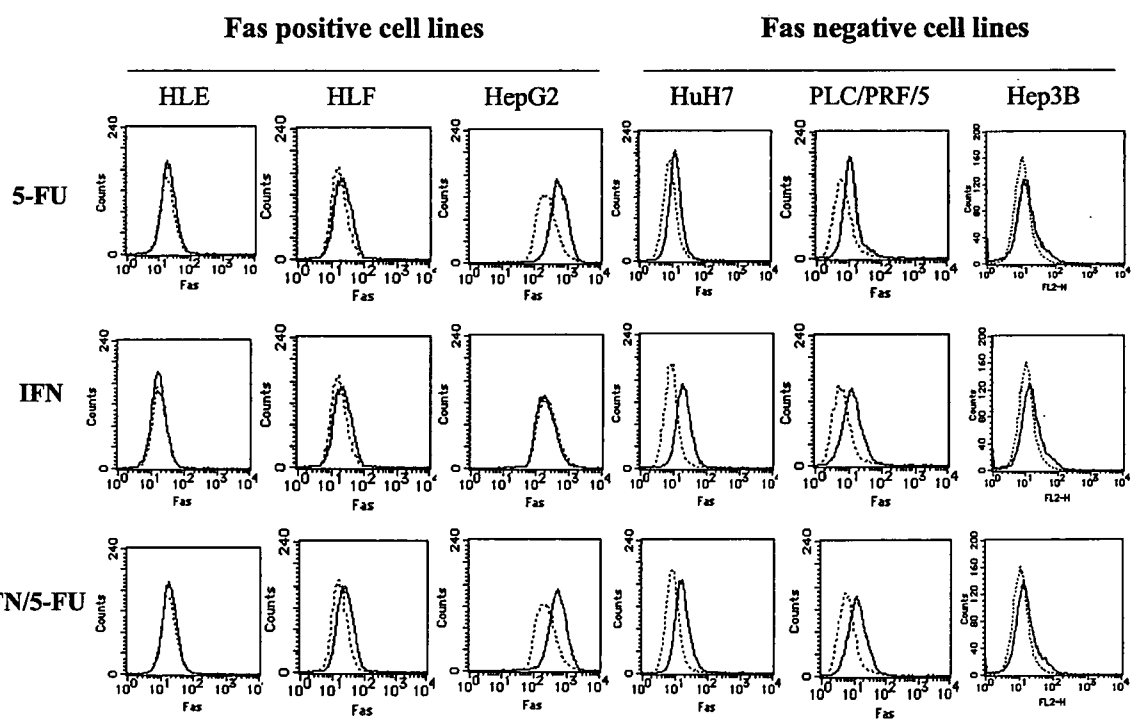

Fig. 4. Regulation of Fas expression induced by IFNα and/or 5-FU. Adherent cells were incubated with IFNα (500 U/ml) and/or 5-FU (0.5 μg/ml) for 24 h. Cell surface Fas was detected by flow cytometry using a mouse monoclonal anti-human Fas IgG (UB2). Histogram with dotted line shows untreated; histogram with solid line represents the drug-treated cells.

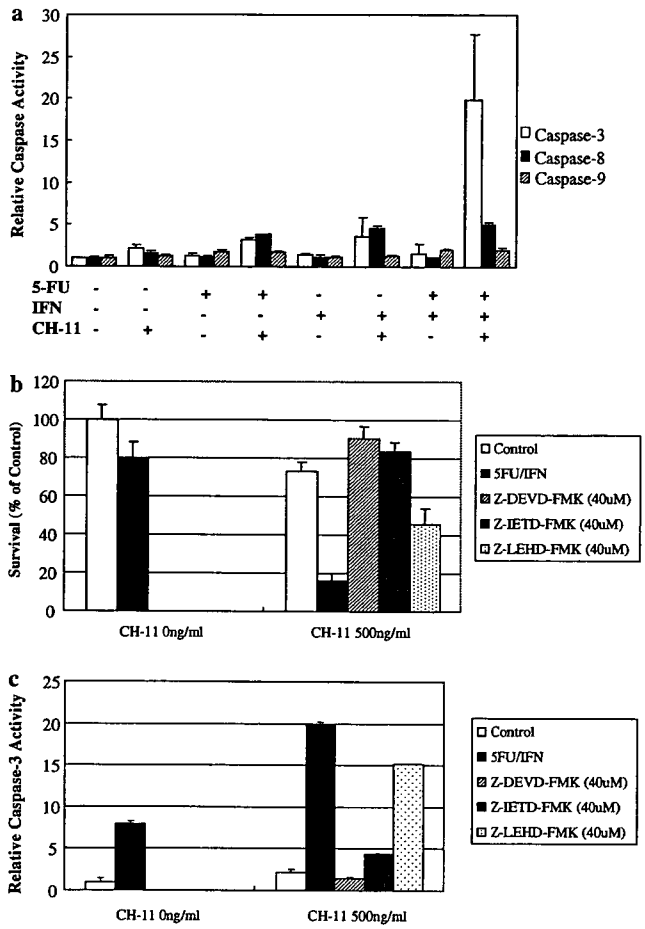

Fig. 5. (a) Activation of caspase-3, -8 and -9 assessed using the Caspase Colorimetric Protease Assay Kit. Data are given relative to results for untreated HepG2 cells. The activity of caspase-3 after 12 h CH-11 (500 ng/ml) treatment was significantly increased by IFNα (500 U/ml) and 5-FU (0.5 μg/ml) alone, but the maximal effect of the CH-11 antibody was observed with the combination of IFNα and 5-FU. (b) Apoptosis blocking effect of specific caspase inhibitors (40 μM) was examined by 48 h MTT assay. Z-DEVD-FMK and Z-IETD-FMK almost totally blocked CH-11 induced apoptosis enhanced by IFNα/5-FU. (c) Colorimetric caspase assay using specific caspase inhibitors (40 μM) was performed. Z-DEVD-FMK inhibited caspase-3 activation induced by CH-11 and IFNα/5-FU. Experiments were performed three times independently. Results represent mean values of three experiments ± SD.

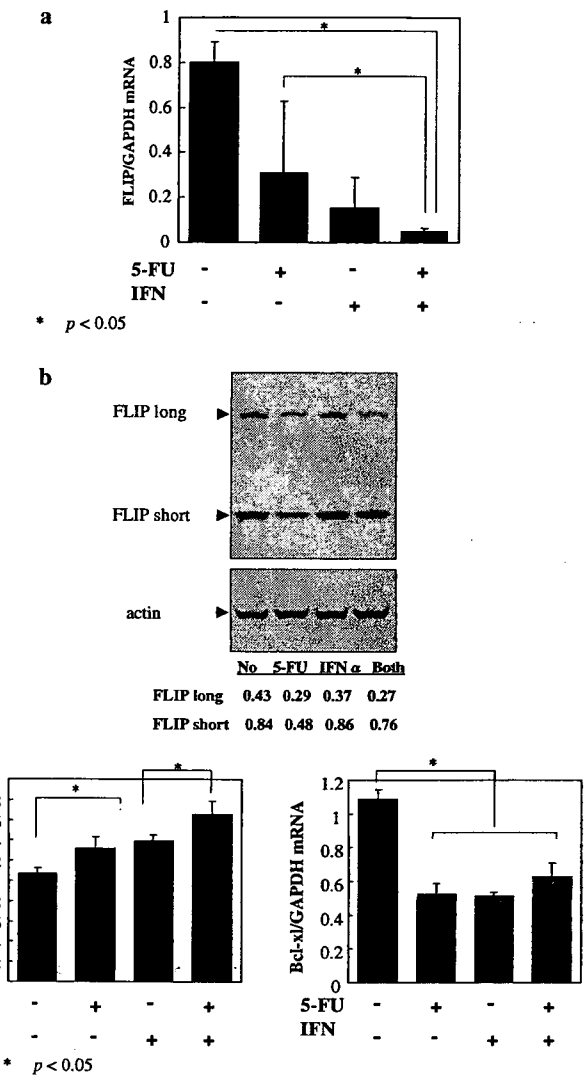

Fig. 6. (a) Expression of FLIP mRNA by RT-PCR. Combination of IFNα (500 U/ml) and 5-FU (0.5 μg/ml) significantly decreased the expression of FLIP mRNA. (b) Western blot analysis of FLIP. Expression of FLIP was decreased by IFNα (500 U/ml) and 5-FU (0.5 μg/ml) in the protein level. (c) Expression of apoptotic factors at mRNA level. Results represent mean values of three experiments ± SD.

and saw an increase in released ^{51}Cr and maximum interaction between effecter cells and target cells. This enhancement was markedly blocked by ZB4 (Fig. 7e).

3.9. Influences of IFNα/5-FU to the normal hepatocyte

MTT assay and TUNEL assay were performed using non-tumorigenic SV40-immortalized human liver epithelial cell line (THLE-2). CH-11 inhibited the cell growth of THLE-2 in the dose-dependent manner (Fig. 8a). But IFNα/5-FU did not affect this growth inhibiting effect (Fig. 8b); and TUNEL assay showed IFNα/5-FU did not increase the CH-11 related apoptosis at all (Fig. 8c). These results suggested that THLE-2 has the sensitivity to Fas/FasL-mediated apoptosis, IFNα/5-FU did not enhance that effect. Concerning these results, TUNEL staining of resected liver specimens was performed. The patients of these specimens received IFNα and 5-FU therapy before the surgery. In the normal tissue, TUNEL-positive cells were very few (Fig. 8, i and iii); there were many TUNEL-positive cells in the tumor site (Fig. 8, ii and iv), as shown in Fig. 8.

4. Discussion

Fas (CD95/Apo-1) belongs to the tumor necrosis factor receptor family of proteins that are expressed at the cell surface in various normal and neoplastic cells [24–

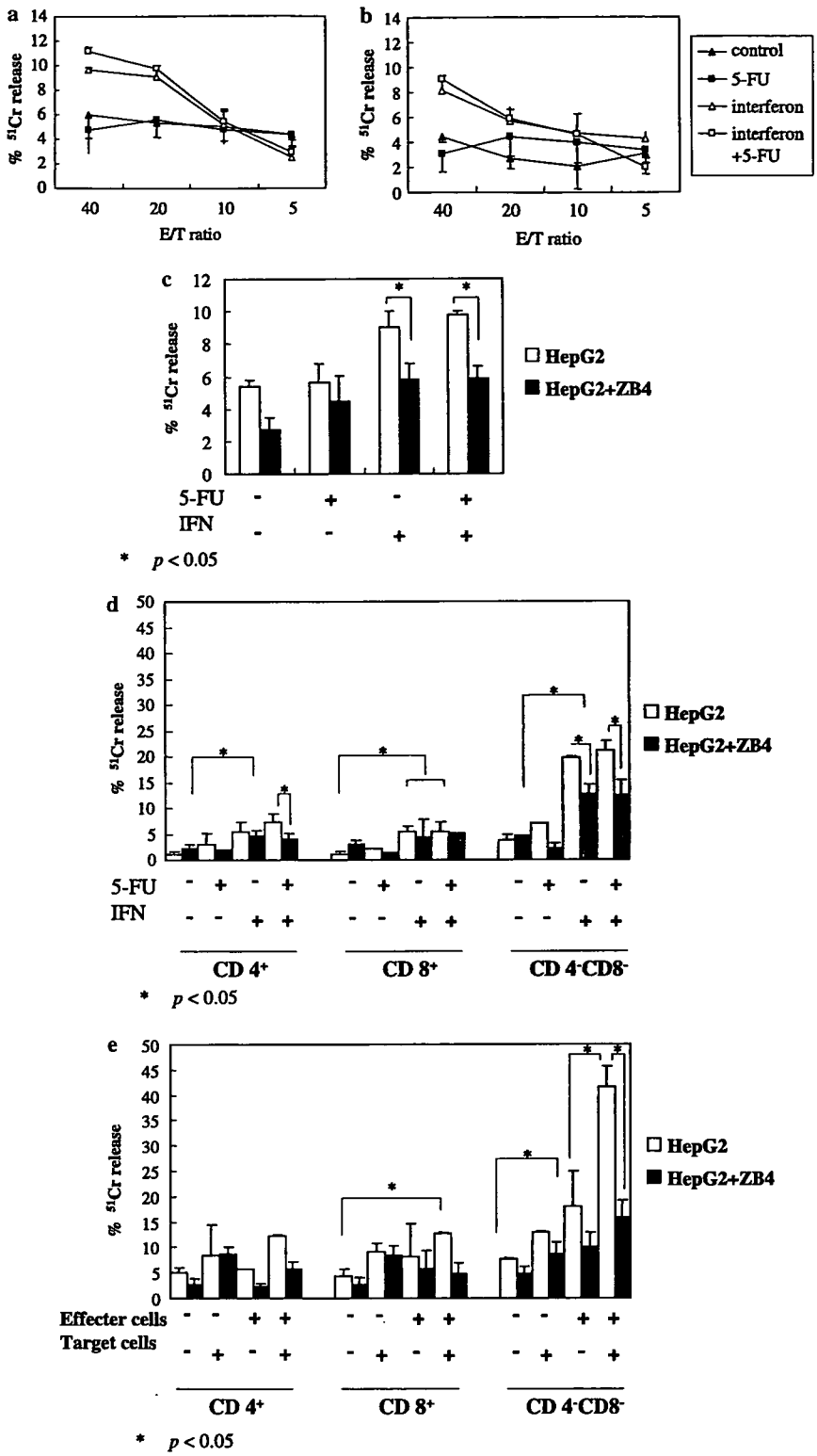

Fig. 7. Cytotoxicity of PBMCs assessed by the 8-h ^{51}Cr-release assay. (a) HepG2 cells were used as target cells. PBMCs stimulated with IFNα (500 U/ml) and/or 5-FU (0.5 μg/ml) for 24 h were used as effecter cells at *E/T* ratios as indicated, without neutralizing anti-Fas antibody, ZB4. (b) The target cells were pretreated with ZB4 (500 ng/ml). (c) Results with an *E/T* ratio of 20. Open bar, without ZB4. Solid bar, with ZB4. (d) CD4$^+$ cells, CD8$^+$ cells, and CD4$^-$CD8$^-$ cells purified from PBMCs using magnetic sorting were used as effecter cells at an *E/T* ratio of 20. (e) Effecter or target cells or both were pretreated with IFNα (500 U/ml) and 5-FU (0.5 μg/ml) for 24 h and an 8-h ^{51}Cr-release assay was performed. All data represent means ± SD values of at least triplicate samples. Similar results were observed in three independent experiments.

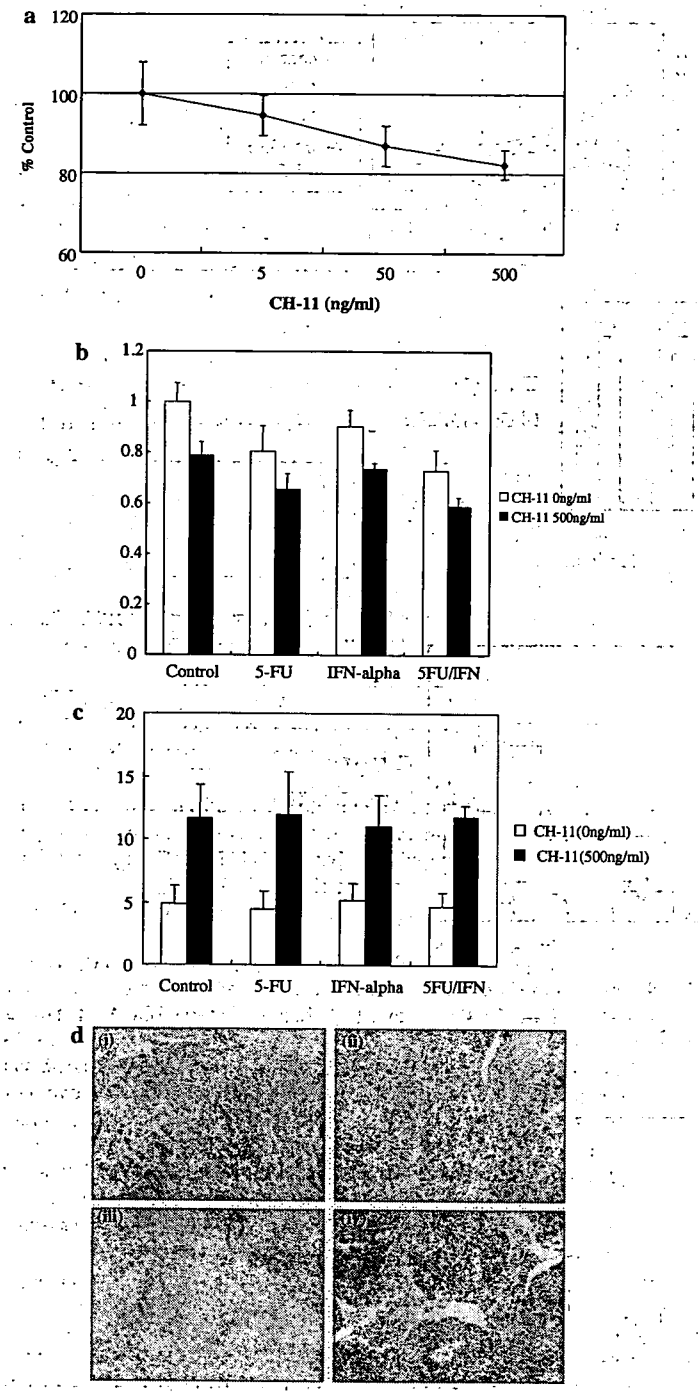

Fig. 8. Hepatotoxicity of IFNα/5-FU was examined using normal hepatocyte cell line THLE-2 and resected human samples. (a) THLE-2 showed sensitivity to CH-11 in the dose-dependent manner in 48 h MTT assay. (b) THLE-2 were incubated with IFNα (500 U/ml) and/or 5-FU (0.5 μg/ml) and with agonistic anti-Fas monoclonal antibody CH-11 (500 ng/ml) (□) or without CH-11 (■) for 48 h. THLE-2 showed sensitivity to IFNα and/or 5-FU or CH-11, but no synergistic effect was observed. (c) TUNEL assay was performed in the same condition with MTT assay. Apoptotic cells were not increased with the stimulation of IFNα and/or 5-FU (d) TUNEL staining of resected samples who received IFNα/5-FU therapy preoperatively (original magnification 100). (i) Normal liver tissues; (ii) tumor site of the specimen; (iii and iv) normal and tumor site of the other patient. TUNEL-positive apoptotic cells were only seen in the tumor. There were very few apoptotic cells in the normal liver. [This figure appears in colour on the web.]

26]. Fas is a 45-kDa type I membrane protein receptor that induces apoptosis by triggering a cascade of caspases following ligation with the Fas Ligand (FasL) on the cell surface of T-cells and NK cells, and plays a major role in T-cell-mediated cytotoxicity [27,28]. Fas/FasL signaling also acts to enhance the effect of many chemotherapeutic drugs against various neoplastic cells, including bleomycin, cisplatin, methotrexate, adriamycin, carboplatin and 5-FU [29–33], and Jiang et al. [34] showed that 5-FU increased Fas/FasL pathway-mediated apoptosis in HCC. However, the mechanism by which apoptosis is induced or enhanced by chemotherapeutic agents remains unclear. In the present study, we confirm the apoptotic effect induced synergistically by IFNα and 5-FU via the Fas/FasL pathway in HCC cells in vitro.

In the first step of this study, we investigated the cell growth response of HCC cells treated with IFNα and/or 5-FU. MTT and annexin-V assays showed that the combination of IFNα and 5-FU significantly increased the sensitivity to Fas-mediated apoptosis in three Fas-positive cell lines, and to a greater extent than either drug used alone. This synergy was not mechanistically related to the level of cell surface Fas expression after treatment, although there was good correlation between the level of constitutive cell surface Fas expression and the extent of Fas-mediated apoptosis. The suggestions of Yano et al. [35] may provide an explanation for these results: (i) protective proteins inhibit apoptosis; (ii) intracellular Fas signaling activation does not happen; and, (iii) regulatory mechanisms exist to enhance Fas-mediated apoptosis other than Fas upregulation [35]. Activated caspase-3 is either partially or totally responsible for cleaving the non-caspase death substrates, which eventually leads to cellular and nuclear morphological changes and ultimately to cell death [25,26]. We speculate here that IFNα and 5-FU affected some apoptotic factors thereby regulating caspase-3 and -8. In addition, these caspases are activated by FLIP, a potent inhibitor of Fas-mediated apoptosis, and regulator of the proteolytic cleavage of caspase-8, based on our results [21,22,36]. Our data also indicated that the increase in caspase-3 expression was more profound than that of caspase-8. This difference might be explained by the regulation of IAPs (inhibitors of apoptosis proteins). IAPs are known to block apoptosis induced by a wide spectrum of triggers, and recent studies have shown that IFNα downregulates IAPs [36–40]. Moreover, PCR array analysis using clinical HCC samples revealed that the BIRC4 gene, which encodes IAP, was significant in predicting the response to IFNα/5-FU therapy [41]. These findings therefore suggest that caspase-8, caspase-3 and FLIP might interact to induce Fas-mediated apoptosis after IFNα/5-FU treatment.

The ^{51}Cr-release assay demonstrated that IFNα markedly induced cytotoxicity of PBMCs against the